Discovery of Natural Sphingomyelin Synthase Inhibitors against High Fat Diet-Induced Obesity and its Lipid Metabolism in Mice

(マウスにおける高脂肪食誘発肥満に対する天然スフィンゴミエリン合成酵素阻害剤の発見とその脂質代謝)

A Thesis Submitted for the Degree of

Doctor of Life Science

Muhamad Aqmal Othman

Laboratory of Molecular Chemical Biology
Transdisciplinary of Life Science Course
Graduate School of Life Science
Hokkaido University, Japan

September 2019

Table of Contents

Chapter 3: Malabaricone C as natural sphingomyelin synthase inhibitor against diet-induced obesity and its lipid metabolism in mice

Acknowledgments

Publications

ABBREVIATIONS USED

SMS, sphingomyelin synthase;

SMSr, sphingomyelin synthase related protein;

SMase, sphingomyelinase;

aSMase, acid sphingomyelinase;

nSMase, neutral sphingomyelinase;

CerS, ceramide synthases;

DES 1, dihydroceramide desaturase 1

PC, phosphatidylcholine;

SM, sphingomyelin;

GM3, ganglioside;

DAG, diacylglycerol;

SPT, serine palmitoyltransferase;

C1P, ceramide 1-phosphate;

S1P, sphingosine 1-phosphate;

SK, sphingosine kinase;

AKT, signalling pathway;

ACDase, acid ceramidase.

ND, normal chow diet;

HFD, high fat diet;

PPAR-ɤ, peroxisome proliferator-activated receptor gamma;

CD36, cluster of differentiation;

FAT, fatty acid translocase;

TG, triglycerides;

FFA, free fatty acid;

NBD, N-[6-[(7-nitro-2-1,3-benzoxadiazol-4-yl)amino]hexanoyl];

T2DM, type 2 diabetes mellitus;

OGTT, oral glucose tolerance test;

DAPI, 4',6-diamidino-2-phenylindole.

TNF, tumor necrosis factor;

LDL, low density lipoprotein;

HDL, high density lipoprotein;

GPCR, G-protein coupled receptor;

Sgpp 2, sphingosine-1 phosphate phosphatase 2;

ER, endoplasmic reticulum;

KO, knockout;

JNK, c-Jun N-terminal kinase signalling pathway;

DSS, dextran sodium sulfate;

MEF, mouse embryonic fibroblasts;

IPA, isopropyl alcohol;

HEP G2, liver hepatocellular carcinoma cells;

DMEM, dulbecco's modified eagle's medium;

FBS, fetal bovine serum;

$CDCI_3$, deuterated chloroform;

CD_3OD, deuterated methanol;

C57BL/6J, C57 black 6 inbred strain of laboratory mouse;

Chapter 1

General Introduction

1.1 Sphingolipids

Sphingolipids represent one of the major classes of eukaryotic lipids. Historically, the first sphingolipids were isolated from brain in the late 19th century by Thudicum, who introduced the name 'sphingosin' after the Greek mythical creature, the Sphinx[1]. Sphingolipids are components of all membranes but are particularly abundant in the myelin sheath. It is composed from a backbone of sphingoid bases which are the founding blocks of all sphingolipids, thus the addition or modifications of the polar head group lead to a various member of the sphingolipid family[2]. Major bioactive sphingolipid includes ceramide, sphingosine 1-phosphate (S1P), sphingomyelin (SM) and ganglioside (GM3) which were appreciated as components of the plasma membrane. These sphingolipids are also important as modulators in particularly, apoptosis inducer, second messenger, signal transducer and for phosphokinase activation.(**Figure 1**)[3].

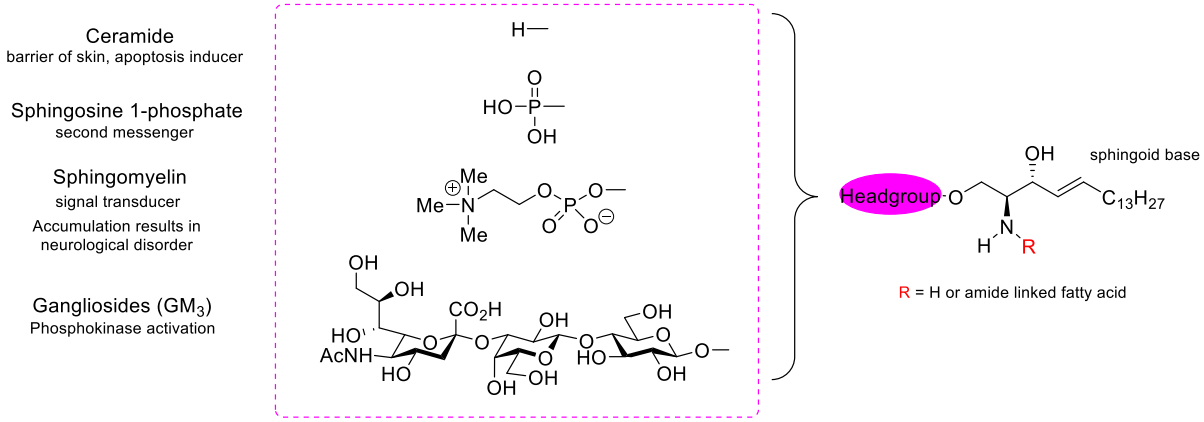

Figure 1: Type of sphingolipids and their main functions

1.2 Sphingolipids metabolism

Sphingolipids are very low in abundance, typically being present in the body at levels of <20% of their glycerolipid counterparts[4,5]. Since bioactive sphingolipids are regulated by various enzymes and fluxes of different metabolites, with around 40 enzymes in mammals involved in their metabolism (**Figure 2**)[6,7]. Complex sphingolipids derive from the addition of various head-groups to a ceramide or dihydroceramide backbone. Pathways of sphingolipid metabolism have become important targets for the development of therapeutics[8]. As ceramide being a major molecule in sphingolipid metabolism & a precursor of complex bioactive sphingolipid, it can be synthesized mainly by 3 pathways.

The initial reaction in the de novo synthesis pathway that produce ceramide involves the decarboxylation of a serine residue and condensation with a fatty acyl-CoA catalysed by serine palmitoyltransferase (SPT)[9,10]. The product of this reaction is 3-ketosphinganine (3-ketodihydrosphingosine). SPT is the rate-limiting enzyme of the sphingolipid biosynthesis pathway. Following formation of 3-ketosphinganine this compound is reduced to sphinganine (dihydrosphingosine) via the action of 3-ketosphinganine reductase (3-ketodihydrosphingosine reductase). Sphinganine is then fatty acylated generating dihydroceramide. The acylation of sphinganine (also called dihydrosphingosine) occurs through the activities of six different ceramide synthases (CerS) in humans. Dihydroceramide is then unsaturated in the original palmitic acid portion of the molecule and forming ceramide by the enzyme dihydroceramide desaturase 1 (DES1).

In sphingolipid salvage pathways, glucosylceramide and sphingosine are converted to ceramide by acid beta glucosidase and ceramide synthase respectively. The last pathway involve in the conversion of ceramide is via sphingomyelin hydrolysis which catalyse by sphingomyelinase[11]. Ceramides are also converted into various complex sphingolipids (predominantly in the Golgi) through modifications at the 1-hydroxyl position to generate ceramide-1-phosphate (C1P), sphingomyelin or glycoceramides, which in turn serve as the precursors for the various glycosphingolipids[12,13]. Constitutive catabolism occurs in the lysosome. Ceramide can then be deacylated to generate sphingosine by ceramidase, which in turn is phosphorylated to sphingosine-1-phosphate (S1P) by sphingosine kinase[14]. Lastly, exit from sphingolipids is initiated by the action of S1P lyase, which cleaves S1P (or dihydroS1P) to a fatty aldehyde and ethanolamine phosphate[15].

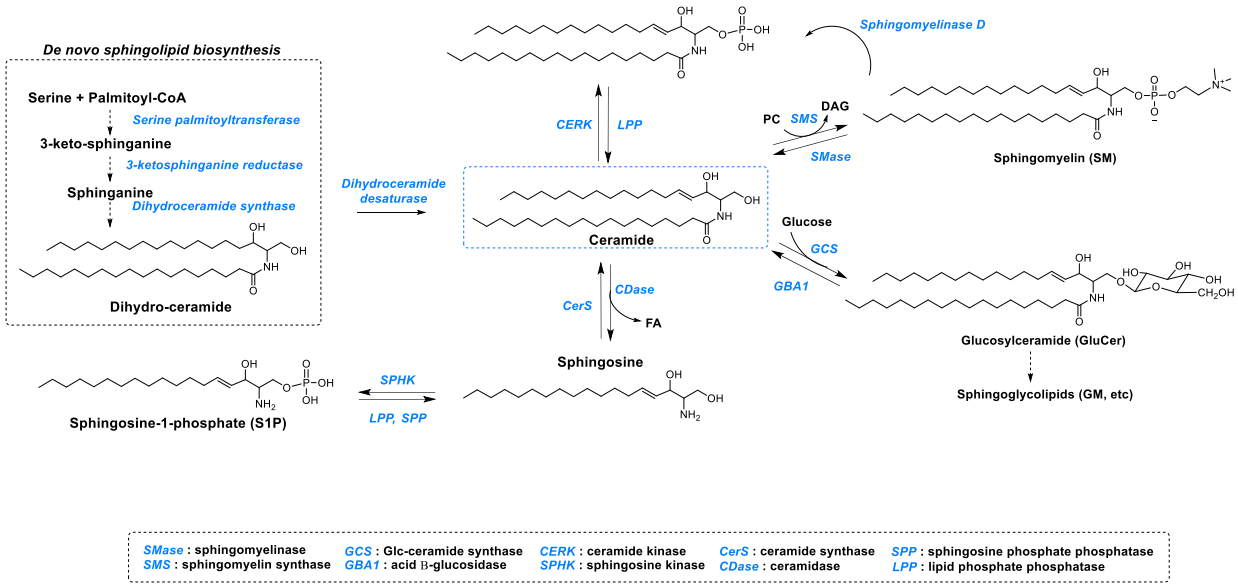

Figure 2: Overview of sphingolipid metabolism.

1.3 Importance of sphingolipids

The main bioactive sphingolipids which received the most attention are ceramide, sphingomyelin and S1P[16,17]. Sphingolipids are also important in cell regulation as modulators of growth factor receptors and as second messengers for a growing list of agonists (including tumor necrosis factor-α, interleukin-1β, nerve growth factor and 1α,25-dihydroxyvitamin D_3). These sphingolipids have been reported to participate in the regulation of cell growth, differentiation, diverse cell functions, and apoptosis[18,19,20]. Considering sphingolipids are major constituents of the plasma membrane, they are also known to form lipid microdomain with cholesterol. This being said, lipid microdomain are also thought to be important not only for signal transduction but also in the absorption of nutrients or lipids from the extracellular space[21]. With regards to this, we focused on sphingolipids in lipid microdomain and their contribution to obesity as well as individual functions of respective sphingolipids.

Ceramide

Ceramide is the precursor for all the complex sphingolipids mentioned earlier and composed of sphingosine and a fatty acid. Numerous studies suggest that ceramides regulate both cell survival and cell death-linked autophagy by regulating nutrient transporters, ER stress and mitophagy[22]. Since then, the cellular activity of ceramide has been extensively studied. Several enzymes that regulate the generation of ceramides, including CerSs, SMases, SK1 and SK2, are distributed in different cellular compartments such as mitochondria, plasma membrane or lysosomes which influence distinct mechanisms of cell death (apoptosis) depending on the activity of these enzymes[23,24].

The levels of ceramide have been shown to be reduced in human colon cancer, consistent with its functions as lipid mediator[25]. Increases in plasma ceramide levels have been shown to be predictive of the response of metastatic tumours to radiation therapy[26]. Furthermore, a strong case is emerging for a role for ceramides in regulating metabolic functions, and changes in levels of ceramide species have been implicated in various metabolic syndromes, such as fatty liver disease[27], obesity[28] and insulin resistance[29]. Cell and *in vivo* studies have demonstrated that increased ceramide levels result in attenuation of insulin action, most likely via inhibition of AKT. This inhibitory pathway appears to be

particularly engaged by the increased supply of palmitic acid, which can drive ceramide synthesis directly as a precursor substrate[29].

Increased ceramide synthesis in the context of insulin resistance was also shown to be driven by inflammatory agents (for example, agonists of Toll-like receptors, TNF and interleukins)[29]. Attenuation of ceramide generation *in vivo*, by use of inhibitors of SPT or dihydroceramide desaturase or mice deficient in these enzymes, improves insulin signalling and glucose and lipid metabolism in diabetes and alleviates obesity-associated metabolic changes and cardiac dysfunction[30,31]. Furthermore, mice deficient in CerS6 are protected from weight gain and glucose intolerance[32] induced by a high-fat diet, and overexpression of ACDase led to a reduction of hepatic steatosis[33].

Sphingolipids, and especially ceramide and sphingosine, have been implicated in vascular disease, including atherosclerosis and ischaemic injury. Increased activity of aSMase and levels of ceramides have been linked to atherogenesis; the mechanism possibly involves secreted aSMase that may act on lipoprotein-associated sphingomyelin to convert it to ceramide[34].

Sphingomyelin

Sphingomyelin (SM) is a key component of the plasma membrane that interacts with cholesterol and glycerophospholipids, thereby participating in the formation and maintenance of lipid microdomains[35]. SM represents about 85% of all sphingolipids in human and it is a major component of plasma membrane lipid (10 to 20%). It is composed of ceramide and a phosphocholine as head group. SM synthesis involves enzymatic transfer of phosphocholine group to a ceramide by sphingomyelin synthase (SMS). The functions of SM are as follows:

1. SM, along with other sphingolipids, are associated with the formation of lipid raft which gives more structural rigidity compared to other part of the plasma membrane lipid bilayer. Excessive SM in the lipid raft may lead to insulin resistance.

2. SM participates in many signalling pathway and it has a significant structural and functional roles in cells. Even though lots of reports support the involvement of SM in signal transduction process the mechanism is still remained elusive[36].

3. SM is the major component of myelin sheath which surrounds and electrically insulates nerve cell axon. The deficiency of sphingomyelin in nerve cells leads to multiple sclerosis which affects the signal transmission process.

The accumulation of SM is found in rare heredity disease called Niemann-pick disease which is caused due to the deficiency of SMase. As a result of this, SM deposition is found in the liver, spleen, lungs, bone marrow and brain lead to irreversible neurological disorders. An excess accumulation sphingomyelin in the blood cell membrane leads to more lipid accumulation in the outer leaflet of the red blood cell membrane which leads to abnormally shaped red cells called acanthocytes. Being the most class found in circulating LDL[37], sphingomyelins which contain saturated acyl-chains are associated with obesity, insulin resistance and decreased liver function in young adults (aged 18–27 years) with obesity[38].

Sphingosine 1-phosphate

S1P has been the most studied bioactive sphingolipid. S1P is mostly secreted from cells and binds to one of five S1PRs, which are G protein-coupled receptors (GPCRs)[39]. These receptors then mediate all known extracellular actions of S1P through canonical GPCR signalling pathways. In addition, a specific pool of S1P bound to high-density lipoprotein (HDL) has been shown to regulate lymphopoiesis and neuroinflammation not only by regulating delivery of S1P to the blood but also by modulating its receptor signalling pathways[40].

On the one hand, S1P has been implicated in tumour cell survival, cancer inflammatory pathways, angiogenesis, resistance to chemotherapy and cancer cell invasion. The SK1–S1P pathway has also been implicated in several other cancers, including glioblastoma, head and neck cancer, renal cancer and several leukaemias[41]. Notably, the cancer-promoting roles of this pathway extend beyond actions on cancer cells (such as protection from apoptosis). For example, S1P has emerged as a key regulator of angiogenesis with widely important implications in vascular biology and cancer[42]. Metabolic roles of S1P are also emerging substantially. In mice, deletion of the gene encoding S1P phosphatase 2 (*Sgpp2*), which degrades S1P, was associated with basal ER stress in pancreatic β-cells and increased sensitivity to a high-fat diet[43]. Consistent with these results, deletion of the gene encoding SK1 was shown to protect against diet-induced hepatic steatosis[44].

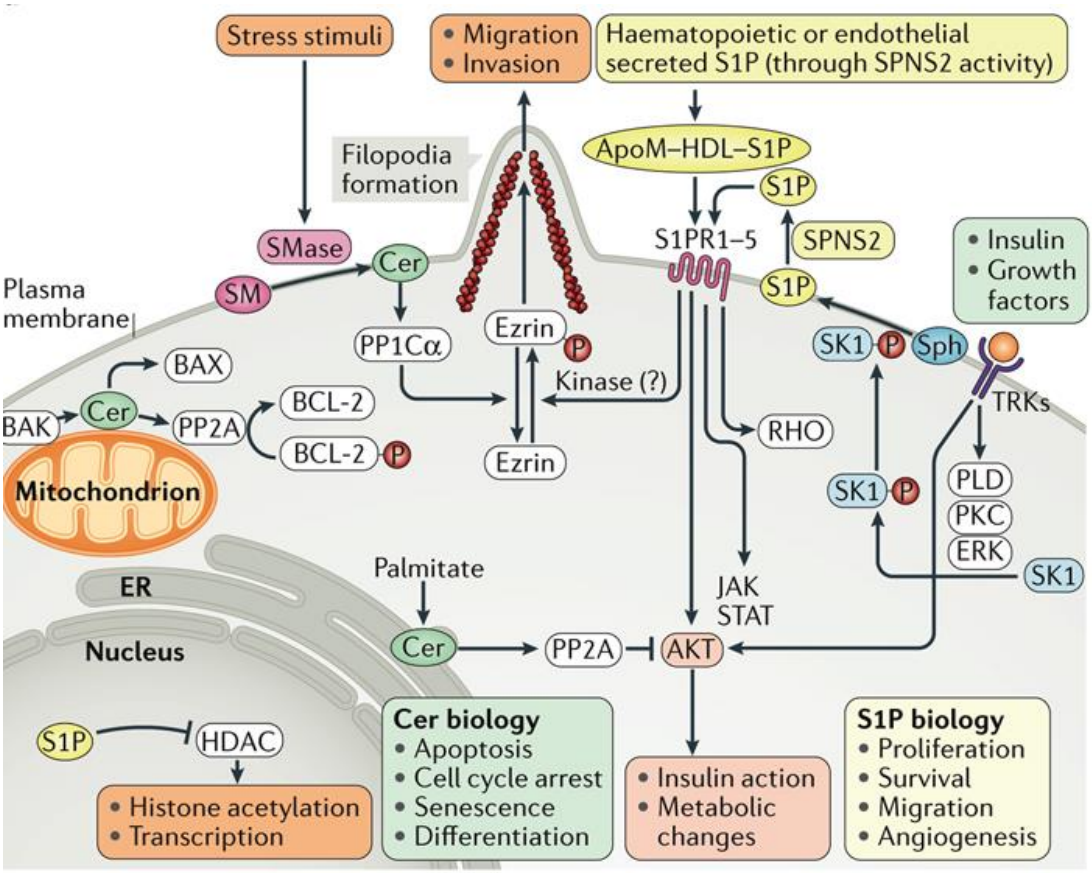

Figure 3: Examples of cellular functions and downstream targets of bioactive sphingolipids.

1.4 Sphingomyelin synthase (SMS) and its related disorders

The gene encoding for sphingomyelin synthase (SMS) was identified in year of 2004. SMS membrane protein family consists of three isoforms, sphingomyelin synthase 1 (SMS1), sphingomyelin synthase 2 (SMS2) and sphingomyelin synthase-related protein (SMSr).[45,46] All three SMSs are six membrane crossing proteins and have both their N- and C- terminus exposed in cytosol (**Figure 4A**). Both SMS 1 and 2, catalyze ceramide and phosphatidylcholine (PC) as substrates to produce sphingomyelin (SM) and diacylglycerol (DAG)[47,48] (**Figure 4B**).

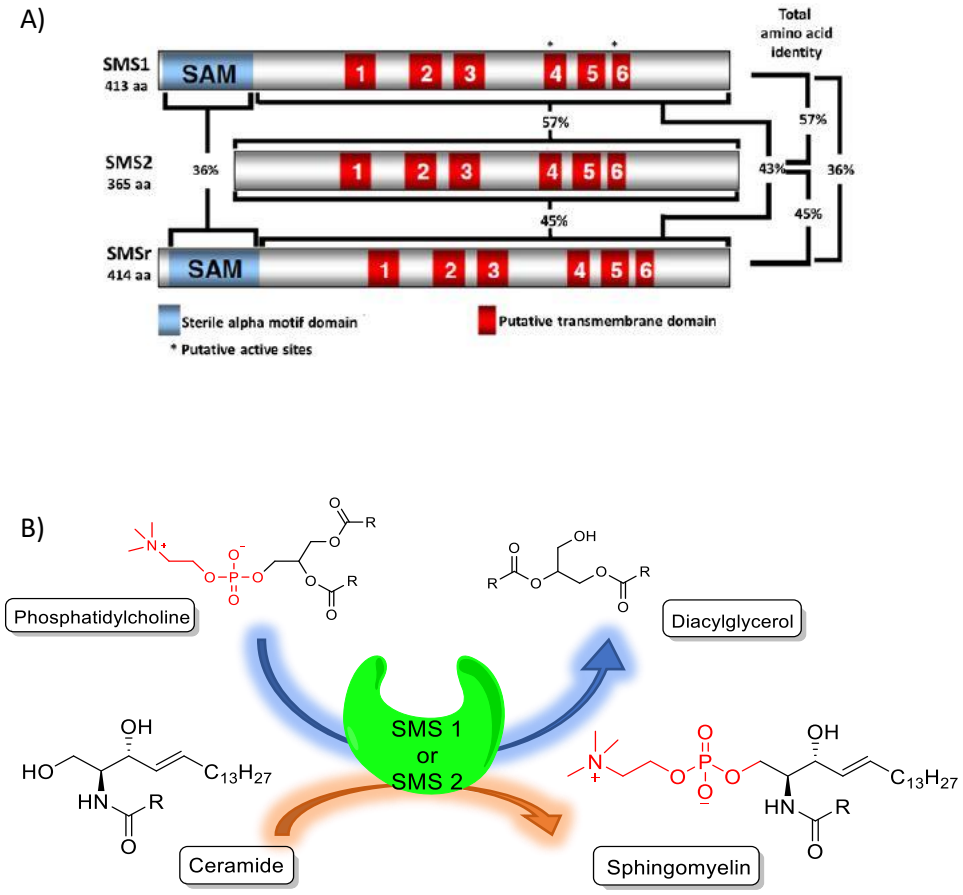

Figure 4: A) Domain architecture of SMS isoforms B) Catalytic conversion of ceramide to sphingomyelin by SMS

SMS1 is responsible for the major SM production in the Golgi apparatus which maintaining cell homeostasis. SMS2 located in the plasma membrane and has a significant role in metabolic related diseases while SMSr is localized in endoplasmic reticulum (ER) which is a suppressor of ceramide-induced mitochondrial apoptosis. The SMSs modulate SM and other sphingolipids levels, thereby regulating membrane fluidity, ceramide-dependent apoptosis, lipid metabolism and signal transduction.[49,50,51,52]

The increasing levels of SM and DAG produced by the SMSs will lead to obesity and insulin resistance.[38,53] SMS knockout mice are resistant to Alzheimer's disease, tumorigenesis, diet-induced obesity, T2DM and are also know to exhibit decreased levels of plasma inflammatory cytokines.[54,55,51,56] Mitsutake et al, recently reported that the deficiency of SMS2 decreases the formation of fatty liver[51]. SMS2 knock out (KO) experiments in high fat diet induced mice results suggest that there is drastic decrease in the deposition of fat around liver compared to wild type (**Figure 5A**). Yuyama et.al also demonstrated that the secretion of neuronal exosomes is modulated by the activities of sphingolipid metabolizing enzymes, neutral sphingomyelinase 2 (nSMase2) and SMS2[54]. Up-regulation of exosome secretion from neuronal cells by treatment of SMS2 siRNA enhanced Aβ uptake into microglial cells and significantly decreased extracellular levels of Aβ (**Figure 5B**).

Furthermore, previous study demonstrated that SMS2-generated DAG in sphingomyelin synthesis inhibits insulin signalling through JNK activation[53] (**Figure 5C**). Very recent study colon cancer and sphingolipid metabolizing enzyme reports SMS2 deficiency inhibits DSS (dextran sodium sulfate)-induced colitis and subsequent colitis-associated colon cancer via inhibition of colon epithelial cell–mediated inflammation[55] (**Figure 5D**).

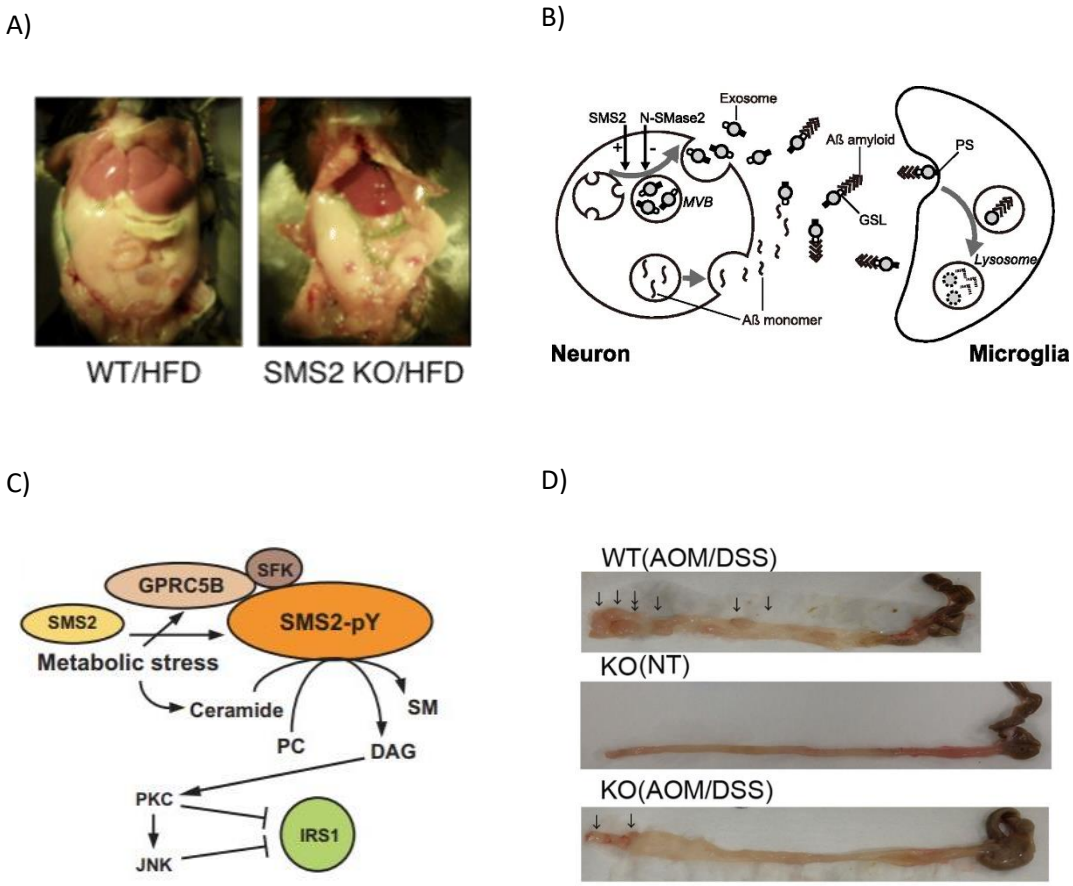

Figure 5: A) SMS2 KO studies of high fat diet induced mouse B) Schematic representation of exosome secretion in Aβ metabolism C) SMS 2- generated DAG cause insulin resistance D) SMS2 inhibition showed decrease in tumour number

1.5 SMS inhibitors and functions

The first compound known as SMS inhibitor is tricyclodecan-9-yl-xanthagenate (D609), which was originally identified as anticancer and antiviral agent[57]. Unfortunately, it is not practically useful because of its less potency towards both SMSs and high instability. Then, a combination of structure-based virtual screening was developed and two compounds were found and identified as D1 and D2 with selectivity towards SMS2[58]. D2 was found to be effective *in vivo* in regulation of ceramide and SM. D2-series SMS inhibitors were synthesized for further optimization but was observed to be unsuitable for a practical drug since their functional moiety, α-aminonitrile, could lead to potential toxicity. In addition, research group from Takeda pharmaceutical company (Japan) able to identify highly potent and selective SMS2 inhibitor **1**, **2** & **3** by synthetic method but their effect towards metabolic diseases are yet to be explored[59]. Indeed, Jaspine B was identified to inhibit the activities of SMSs, but there is no IC_{50} values reported[60]. Therefore, the inhibition of the SMSs enzymes by natural occurring substrates would be an ideal therapeutic approach notably, for metabolic syndrome.

Very recently, the inhibitory activity of Gingkolic acid from the leaves of *Gingko biloba* was reported by our group.[61] Though, Gingkolic acid has been proven to be an effective inhibitor with equal inhibiting potentials (IC_{50} = 1.5 µM) against both enzymes, studies have revealed that Gingkolic acid is toxic, thus making it an unsuitable candidate for the further development of it as a drug (**Figure 6**). Furthermore, there are various report regarding the synthetic SMS inhibitors but most of them showed complex interaction and problems. Since plant kingdom is a major source of drugs, therefore we can expect diverse chemical structures for the prevention and treatment of targeted diseases. On top of that, there is still a few report regarding natural SMS inhibitor, Hence there is a dire need to identify the natural occurring inhibitor with safe and lesser side effects.

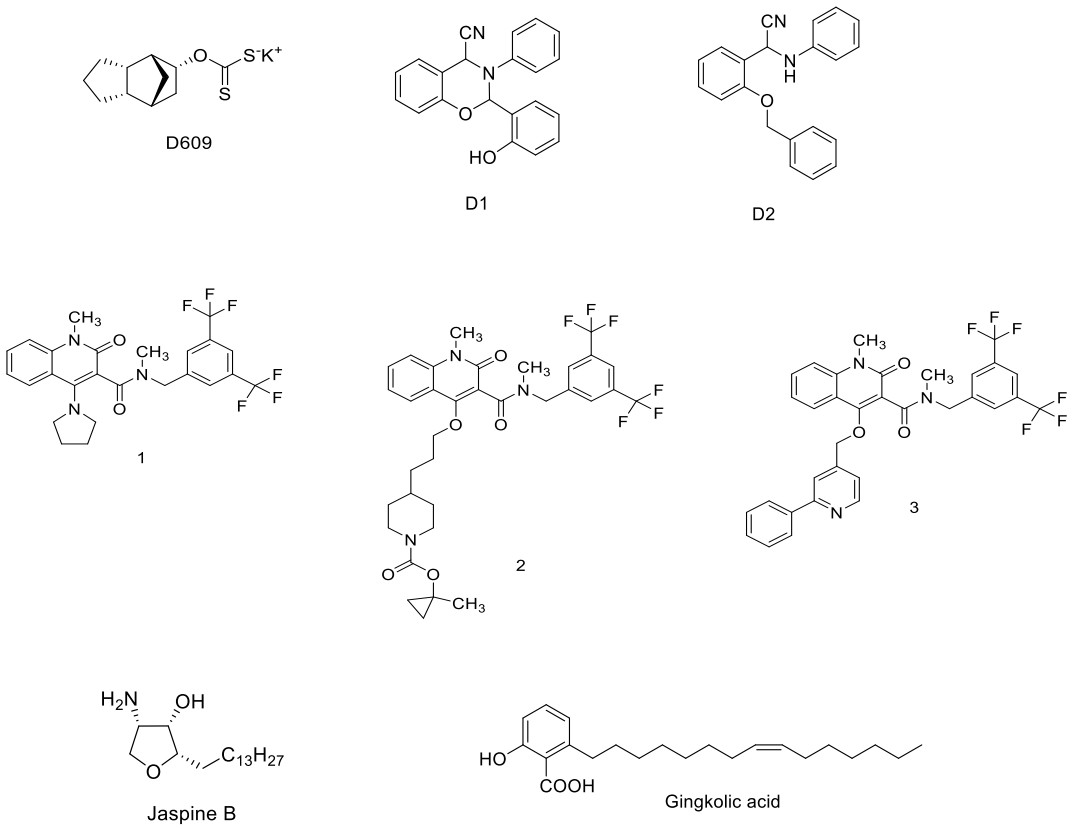

Figure 6: Synthetic and natural SMS inhibitors

1.6 References

(1) Thudichum, J. *A Treatise on the Chemical Constitution of the Brain.*; Archon Books: Hamden Conn., 1962.

(2) Hannun, Y. A.; Obeid, L. M. Sphingolipids and Their Metabolism in Physiology and Disease. *Nat. Rev. Mol. Cell Biol.* **2017**, *19* (3), 175–191.

(3) Merrill, A. H. Sphingolipid and Glycosphingolipid Metabolic Pathways in the Era of Sphingolipidomics. *Chem. Rev.* **2011**, *111* (10), 6387–6422.

(4) Cabukusta, B.; Kol, M.; Kneller, L.; Hilderink, A.; Bickert, A.; Mina, J. G. M.; Korneev, S.; Holthuis, J. C. M. ER Residency of the Ceramide Phosphoethanolamine Synthase SMSr Relies on Homotypic Oligomerization Mediated by Its SAM Domain. *Sci. Rep.* **2017**, *7* (1), 41290.

(5) Adada, M. M.; Canals, D.; Jeong, N.; Kelkar, A. D.; Hernandez-Corbacho, M.; Pulkoski-Gross, M. J.; Donaldson, J. C.; Hannun, Y. A.; Obeid, L. M. Intracellular Sphingosine Kinase 2–derived Sphingosine-1-Phosphate Mediates Epidermal Growth Factor–induced Ezrin-Radixin-Moesin Phosphorylation and Cancer Cell Invasion. *FASEB J.* **2015**, *29* (11), 4654–4669.

(6) Hannun, Y. A.; Obeid, L. M. Many Ceramides. *J. Biol. Chem.* **2011**, *286* (32), 27855–27862.

(7) Schulze, H.; Sandhoff, K. Sphingolipids and Lysosomal Pathologies. *Biochim. Biophys. Acta - Mol. Cell Biol. Lipids* **2014**, *1841* (5), 799–810.

(8) Huang, X.; Withers, B. R.; Dickson, R. C. Sphingolipids and Lifespan Regulation. *Biochim. Biophys. Acta - Mol. Cell Biol. Lipids* **2014**, *1841* (5), 657–664.

(9) Holland, W. L.; Summers, S. A. Sphingolipids, Insulin Resistance, and Metabolic Disease: New Insights from in Vivo Manipulation of Sphingolipid Metabolism. *Endocr. Rev.* **2008**, *29* (4), 381–402.

(10) Merrill, A. H. *De Novo* Sphingolipid Biosynthesis: A Necessary, but Dangerous, Pathway. *J. Biol. Chem.* **2002**, *277* (29), 25843–25846.

(11) Gault, C. R.; Obeid, L. M.; Hannun, Y. A. An Overview of Sphingolipid Metabolism: From Synthesis to Breakdown. *Adv. Exp. Med. Biol.* **2010**, *688*, 1–23.

(12) Hanada, K.; Kumagai, K.; Yasuda, S.; Miura, Y.; Kawano, M.; Fukasawa, M.; Nishijima, M. Molecular Machinery for Non-Vesicular Trafficking of Ceramide. *Nature* **2003**, *426* (6968), 803–809.

(13) Lannert, H.; Bünning, G.; Jeckel, D.; Wieland, F. T. Lactosylceramide Is Synthesized in the Lumen of the Golgi Apparatus. *FEBS Lett.* **1994**, *342* (1), 91–96.

(14) Beckham, T. H.; Cheng, J. C.; Marrison, S. T.; Norris, J. S.; Liu, X. Interdiction of Sphingolipid Metabolism to Improve Standard Cancer Therapies. *Adv. Cancer Res.* **2013**, *117*, 1–36.

(15) Hagen-Euteneuer, N.; Lütjohann, D.; Park, H.; Merrill, A. H.; van Echten-Deckert, G.; Echten-Deckert, G. van. Sphingosine 1-Phosphate (S1P) Lyase Deficiency Increases

Sphingolipid Formation via Recycling at the Expense of de Novo Biosynthesis in Neurons. *J. Biol. Chem.* **2012**, *287* (12), 9128–9136.

(16) Futerman, A. H.; Hannun, Y. A. The Complex Life of Simple Sphingolipids. *EMBO Rep.* **2004**, *5* (8), 777–782.

(17) Bartke, N.; Hannun, Y. A. Bioactive Sphingolipids: Metabolism and Function. *J. Lipid Res.* **2009**, *50* (Suppl), S91.

(18) Merrill, A. H.; Liotta, D. C.; Riley, R. T. Sphingolipids as Regulators of Cellular Growth, Differentiation, and Behavior. *Adv. Lipobiology* **1996**, *1*, 273–298.

(19) Merrill, A. H.; Schmelz, E.-M.; Wang, E.; Dillehay, D. L.; Rice, L. G.; Meredith, F.; Riley, R. T. Importance of Sphingolipids and Inhibitors of Sphingolipid Metabolism as Components of Animal Diets. *J. Nutr.* **1997**, *127* (5), 830S–833S.

(20) Young, S. A.; Mina, J. G.; Denny, P. W.; Smith, T. K. Sphingolipid and Ceramide Homeostasis: Potential Therapeutic Targets. *Biochem. Res. Int.* **2012**, *2012*, 1–12.

(21) Cheng, Z.-J.; Deep Singh, R.; Marks, D. L.; Pagano, R. E. Membrane Microdomains, Caveolae, and Caveolar Endocytosis of Sphingolipids (Review). *Mol. Membr. Biol.* **2006**, *23* (1), 101–110.

(22) Dany, M.; Ogretmen, B. Ceramide Induced Mitophagy and Tumor Suppression. *Biochim. Biophys. Acta - Mol. Cell Res.* **2015**, *1853* (10), 2834–2845.

(23) Jain, A.; Beutel, O.; Ebell, K.; Korneev, S.; Holthuis, J. C. M. Diverting CERT-Mediated Ceramide Transport to Mitochondria Triggers Bax-Dependent Apoptosis. *J. Cell Sci.* **2017**, *130* (2), 360–371.

(24) Siskind, L. J.; Mullen, T. D.; Romero Rosales, K.; Clarke, C. J.; Hernandez-Corbacho, M. J.; Edinger, A. L.; Obeid, L. M. The BCL-2 Protein BAK Is Required for Long-Chain Ceramide Generation during Apoptosis. *J. Biol. Chem.* **2010**, *285* (16), 11818–11826.

(25) García-Barros, M.; Coant, N.; Kawamori, T.; Wada, M.; Snider, A. J.; Truman, J.-P.; Wu, B. X.; Furuya, H.; Clarke, C. J.; Bialkowska, A. B.; et al. Role of Neutral Ceramidase in Colon Cancer. *FASEB J.* **2016**, *30* (12), 4159–4171.

(26) Dubois, N.; Rio, E.; Ripoche, N.; Ferchaud-Roucher, V.; Gaugler, M.-H.; Campion, L.; Krempf, M.; Carrie, C.; Mahé, M.; Mirabel, X.; et al. Plasma Ceramide, a Real-Time Predictive Marker of Pulmonary and Hepatic Metastases Response to Stereotactic Body Radiation Therapy Combined with Irinotecan. *Radiother. Oncol.* **2016**, *119* (2), 229–235.

(27) Kasumov, T.; Li, L.; Li, M.; Gulshan, K.; Kirwan, J. P.; Liu, X.; Previs, S.; Willard, B.; Smith, J. D.; McCullough, A. Ceramide as a Mediator of Non-Alcoholic Fatty Liver Disease and Associated Atherosclerosis. *PLoS One* **2015**, *10* (5), e0126910.

(28) Boini, K. M.; Zhang, C.; Xia, M.; Poklis, J. L.; Li, P.-L. Role of Sphingolipid Mediator Ceramide in Obesity and Renal Injury in Mice Fed a High-Fat Diet. *J. Pharmacol. Exp. Ther.* **2010**, *334* (3), 839–846.

(29) Chaurasia, B.; Summers, S. A. Ceramides – Lipotoxic Inducers of Metabolic Disorders. *Trends Endocrinol. Metab.* **2015**, *26* (10), 538–550.

(30) Hodson, A. E.; Tippetts, T. S.; Bikman, B. T. Insulin Treatment Increases Myocardial Ceramide Accumulation and Disrupts Cardiometabolic Function. *Cardiovasc. Diabetol.* **2015**, *14* (1), 153.

(31) Kurek, K.; Wiesiołek-Kurek, P.; Piotrowska, D. M.; Łukaszuk, B.; Chabowski, A.; Żendzianendzian-Piotrowska, M. Inhibition of Ceramide de Novo Synthesis with Myriocin Affects Lipid Metabolism in the Liver of Rats with Streptozotocin-Induced Type 1 Diabetes. *Biomed Res. Int.* **2014**, *2014*, 980815.

(32) Turpin, S. M.; Nicholls, H. T.; Willmes, D. M.; Mourier, A.; Brodesser, S.; Wunderlich, C. M.; Mauer, J.; Xu, E.; Hammerschmidt, P.; Brönneke, H. S.; et al. Obesity-Induced CerS6-Dependent C16:0 Ceramide Production Promotes Weight Gain and Glucose Intolerance. *Cell Metab.* **2014**, *20* (4), 678–686.

(33) Xia, J. Y.; Holland, W. L.; Kusminski, C. M.; Sun, K.; Sharma, A. X.; Pearson, M. J.; Sifuentes, A. J.; McDonald, J. G.; Gordillo, R.; Scherer, P. E. Targeted Induction of Ceramide Degradation Leads to Improved Systemic Metabolism and Reduced Hepatic Steatosis. *Cell Metab.* **2015**, *22* (2), 266–278.

(34) Hirsch, E.; Irikura, V. M.; Paul, S. M.; Hirsh, D.; Marathe, S.; Johns, A.; Gold, P. W.; Hirsch, E.; Williams, K. J.; Licinio, J.; et al. Functions of Interleukin 1 Receptor Antagonist in Gene Knockout and Overproducing Mice. *Proc. Natl. Acad. Sci. U. S. A.* **1996**, *93* (20), 11008–11013.

(35) Barceló-Coblijn, G.; Martin, M. L.; de Almeida, R. F. M.; Noguera-Salvà, M. A.; Marcilla-Etxenike, A.; Guardiola-Serrano, F.; Lüth, A.; Kleuser, B.; Halver, J. E.; Escribá, P. V. Sphingomyelin and Sphingomyelin Synthase (SMS) in the Malignant Transformation of Glioma Cells and in 2-Hydroxyoleic Acid Therapy. *Proc. Natl. Acad. Sci. U. S. A.* **2011**, *108* (49), 19569–19574.

(36) Chakraborty, M.; Jiang, X.-C. Sphingomyelin and Its Role in Cellular Signaling; Springer, Dordrecht, 2013; pp 1–14.

(37) Meikle, P. J.; Wong, G.; Tan, R.; Giral, P.; Robillard, P.; Orsoni, A.; Hounslow, N.; Magliano, D. J.; Shaw, J. E.; Curran, J. E.; et al. Statin Action Favors Normalization of the Plasma Lipidome in the Atherogenic Mixed Dyslipidemia of MetS: Potential Relevance to Statin-Associated Dysglycemia. *J. Lipid Res.* **2015**, *56* (12), 2381–2392.

(38) Hanamatsu, H.; Ohnishi, S.; Sakai, S.; Yuyama, K.; Mitsutake, S.; Takeda, H.; Hashino, S.; Igarashi, Y. Altered Levels of Serum Sphingomyelin and Ceramide Containing Distinct Acyl Chains in Young Obese Adults. *Nutr. Diabetes* **2014**, *4* (10), e141.

(39) Sanchez, T.; Hla, T. Structural and Functional Characteristics of S1P Receptors. *J. Cell. Biochem.* **2004**, *92* (5), 913–922.

(40) Blaho, V. A.; Galvani, S.; Engelbrecht, E.; Liu, C.; Swendeman, S. L.; Kono, M.; Proia, R. L.; Steinman, L.; Han, M. H.; Hla, T. HDL-Bound Sphingosine-1-Phosphate Restrains Lymphopoiesis and Neuroinflammation. *Nature* **2015**, *523* (7560), 342–346.

(41) Heffernan-Stroud, L. A.; Obeid, L. M. Sphingosine Kinase 1 in Cancer. *Adv. Cancer Res.* **2013**, *117*, 201–235.

(42) Nagahashi, M.; Hait, N. C.; Maceyka, M.; Avni, D.; Takabe, K.; Milstien, S.; Spiegel, S. Sphingosine-1-Phosphate in Chronic Intestinal Inflammation and Cancer. *Adv. Biol.*

Regul. **2014**, *54*, 112–120.

(43) Taguchi, Y.; Allende, M. L.; Mizukami, H.; Cook, E. K.; Gavrilova, O.; Tuymetova, G.; Clarke, B. A.; Chen, W.; Olivera, A.; Proia, R. L. Sphingosine-1-Phosphate Phosphatase 2 Regulates Pancreatic Islet β-Cell Endoplasmic Reticulum Stress and Proliferation. *J. Biol. Chem.* **2016**, *291* (23), 12029–12038.

(44) Chen, J.; Wang, W.; Qi, Y.; Kaczorowski, D.; McCaughan, G. W.; Gamble, J. R.; Don, A. S.; Gao, X.; Vadas, M. A.; Xia, P. Deletion of Sphingosine Kinase 1 Ameliorates Hepatic Steatosis in Diet-Induced Obese Mice: Role of PPARγ. *Biochim. Biophys. Acta - Mol. Cell Biol. Lipids* **2016**, *1861* (2), 138–147.

(45) Huitema, K.; van den Dikkenberg, J.; Brouwers, J. F. H. M.; Holthuis, J. C. M. Identification of a Family of Animal Sphingomyelin Synthases. *EMBO J.* **2004**, *23* (1), 33–44.

(46) Yamaoka, S.; Miyaji, M.; Kitano, T.; Umehara, H.; Okazaki, T. Expression Cloning of a Human CDNA Restoring Sphingomyelin Synthesis and Cell Growth in Sphingomyelin Synthase-Defective Lymphoid Cells. *J. Biol. Chem.* **2004**, *279* (18), 18688–18693.

(47) Ullman, M. D.; Radin, N. S. The Enzymatic Formation of Sphingomyelin from Ceramide and Lecithin in Mouse Liver. *J. Biol. Chem.* **1974**, *249* (5), 1506–1512.

(48) Merrill, A. H.; Jones, D. D. An Update of the Enzymology and Regulation of Sphingomyelin Metabolism. *Biochim. Biophys. Acta - Lipids Lipid Metab.* **1990**, *1044* (1), 1–12.

(49) Bienias, K.; Fiedorowicz, A.; Sadowska, A.; Prokopiuk, S.; Car, H. Regulation of Sphingomyelin Metabolism. *Pharmacol. Reports* **2016**, *68* (3), 570–581.

(50) Hannun, Y. A. Functions of Ceramide in Coordinating Cellular Responses to Stress. *Science* **1996**, *274* (5294), 1855–1859.

(51) Mitsutake, S.; Zama, K.; Yokota, H.; Yoshida, T.; Tanaka, M.; Mitsui, M.; Ikawa, M.; Okabe, M.; Tanaka, Y.; Yamashita, T.; et al. Dynamic Modification of Sphingomyelin in Lipid Microdomains Controls Development of Obesity, Fatty Liver, and Type 2 Diabetes. *J. Biol. Chem.* **2011**, *286* (32), 28544–28555.

(52) Yuyama, K.; Sun, H.; Mitsutake, S.; Igarashi, Y. Sphingolipid-Modulated Exosome Secretion Promotes Clearance of Amyloid-β by Microglia. *J. Biol. Chem.* **2012**, *287* (14), 10977–10989.

(53) Kim, Y.-J.; Greimel, P.; Hirabayashi, Y. GPRC5B-Mediated Sphingomyelin Synthase 2 Phosphorylation Plays a Critical Role in Insulin Resistance. *iScience* **2018**, *8*, 250–266.

(54) Yuyama, K.; Mitsutake, S.; Igarashi, Y. Pathological Roles of Ceramide and Its Metabolites in Metabolic Syndrome and Alzheimer's Disease. *Biochim. Biophys. Acta - Mol. Cell Biol. Lipids* **2014**, *1841* (5), 793–798.

(55) Ohnishi, T.; Hashizume, C.; Taniguchi, M.; Furumoto, H.; Han, J.; Gao, R.; Kinami, S.; Kosaka, T.; Okazaki, T. Sphingomyelin Synthase 2 Deficiency Inhibits the Induction of Murine Colitis-Associated Colon Cancer. *FASEB J.* **2017**, *31* (9), 3816–3830.

(56) Fan, Y.; Shi, F.; Liu, J.; Dong, J.; Bui, H. H.; Peake, D. A.; Kuo, M.-S.; Cao, G.; Jiang, X.-C. Selective Reduction in the Sphingomyelin Content of Atherogenic Lipoproteins Inhibits Their Retention in Murine Aortas and the Subsequent Development of Atherosclerosis. *Arterioscler. Thromb. Vasc. Biol.* **2010**, *30* (11), 2114–2120.

(57) Kiss, Z.; Tomono, M. Compound D609 Inhibits Phorbol Ester-Stimulated Phospholipase D Activity and Phospholipase C-Mediated Phosphatidylethanolamine Hydrolysis. *Biochim. Biophys. Acta - Lipids Lipid Metab.* **1995**, *1259* (1), 105–108.

(58) Deng, X.; Lin, F.; Zhang, Y.; Li, Y.; Zhou, L.; Lou, B.; Li, Y.; Dong, J.; Ding, T.; Jiang, X.; et al. Identification of Small Molecule Sphingomyelin Synthase Inhibitors. *Eur. J. Med. Chem.* **2014**, *73*, 1–7.

(59) Adachi, R.; Ogawa, K.; Matsumoto, S.; Satou, T.; Tanaka, Y.; Sakamoto, J.; Nakahata, T.; Okamoto, R.; Kamaura, M.; Kawamoto, T. Discovery and Characterization of Selective Human Sphingomyelin Synthase 2 Inhibitors. *Eur. J. Med. Chem.* **2017**, *136*, 283–293.

(60) Salma, Y.; Lafont, E.; Therville, N.; Carpentier, S.; Bonnafé, M. J.; Levade, T.; Génisson, Y.; Andrieu-Abadie, N. The Natural Marine Anhydrophytosphingosine, Jaspine B, Induces Apoptosis in Melanoma Cells by Interfering with Ceramide Metabolism. *Biochem. Pharmacol.* **2009**, *78* (5), 477–485.

(61) Swamy, M. M. M.; Murai, Y.; Ohno, Y.; Jojima, K.; Kihara, A.; Mitsutake, S.; Igarashi, Y.; Yu, J.; Yao, M.; Suga, Y.; et al. Structure-Inspired Design of a Sphingolipid Mimic Sphingosine-1-Phosphate Receptor Agonist from a Naturally Occurring Sphingomyelin Synthase Inhibitor. *Chem. Commun.* **2018**, *54* (90), 12758–12761.

Chapter 2

Natural sphingomyelin synthase (SMS) inhibitors from various medicinal plants and free fatty acids.

2.1 Abstract

Sphingomyelin synthase (SMS) membrane protein family catalyze ceramide and phosphatidylcholine (PC) as substrates to produce sphingomyelin (SM) and diacylglycerol (DAG). The SMSs modulate SM and other sphingolipids levels, thereby regulating membrane fluidity, ceramide-dependent apoptosis, lipid metabolism and signal transduction. The increasing levels of SM and DAG produced by the SMSs will lead to obesity and insulin resistance. In search of identifying new scaffold for SMS inhibitor, we screened a library of medicinal plant extracts. As a result, we manage to identify 13 promising natural SMSs inhibitors. Both fluorescence substrates, phosphocholine and ceramide were utilized to better understanding the selectivity of catalysation reaction by SMSs. A series of free fatty acids composed of both saturated and unsaturated were screened against SMSs to discover its functional food properties. The promising functional food properties would be a suitable alternative in search of supplements which can be employed in the treatment and prevention of SMSs related diseases.

2.2 Introduction

Sphingomyelin synthase (SMS) membrane protein catalyze ceramide and phosphatidylcholine (PC) as substrates to produce sphingomyelin (SM) and diacylglycerol (DAG).[1,2] The SMSs modulate SM and other sphingolipids levels, thereby regulating membrane fluidity, ceramide-dependent apoptosis, lipid metabolism and signal transduction.[3,4,5,6] The increasing levels of SM and DAG produced by the SMSs will lead to obesity and insulin resistance.[7,8] SMS knockout mice are resistant to Alzheimer's disease, tumorigenesis, diet-induced obesity, T2DM and are also know to exhibit decreased levels of plasma inflammatory cytokines.[9,10,5,11]

Development of metabolic related diseases have multiple causes, and yet there is no single treatment available. Pharmacological approach which introduce separate drugs for each disease has various side effects. New alternative need to be introduced to solve this problem. Therefore, the inhibition of the SMS 1 and SMS 2 enzymes would be an ideal approach in reducing the levels of SM and DAG. Employing plant derived natural products for this purpose would be a suitable strategy.

Little is known about the use of secondary metabolites from plants, culinary herbs, spices, vegetables and fruits as SMS 1 and SMS 2 inhibitors. Since the plant kingdom is a major source of drugs, therefore we can expect diverse chemical structures from their secondary metabolites for the purpose of drug discovery. This being said, as SMSs consists of two substrates involved in their catalyzation reaction, a thorough literature review has revealed that there is no report regarding the natural inhibitors which possess dual inhibition effects. Hence, this prompted us to conduct a thorough screening investigation using both fluorescence substrates NBD-phosphocholine and NBD- ceramide in search of the potency to the SMSs inhibition and to better understand the mechanism behind it.

On the other hand, a series of free fatty acids were also screened to identify the specificity of the SMSs inhibition. Though, various free fatty acids have been proven to be an important component of human body especially omega 3, 6 and 9, the functions of fatty acids still remains unknown for the SMSs inhibition activity. With regard to this, in the present work, we report the screening of unsaturated and saturated fatty acids to discover their inhibiting potential in order to understand the specific inhibition which involved the membrane protein.

2.3 Results and discussion

To search for active medicinal plants that inhibit SMS enzyme, our group initiated a screening to identify SMS inhibitor from more than 650 crude extract libraries.[12] Screening results showed only 5 extracts were identified with good inhibition against target enzymes which were *Myristica cinnamomea*, *Chamaecyparis pisifera var filifera*, *Dryopteris crassirhizoma*, *Morus bombycis* and *Walsura pinnata* (**Scheme 1**). To determine active natural compounds which responsible for the inhibition, a bioassay-guided procedure was implemented for all active extracts and resulted in 13 natural inhibitors against SMS1 & SMS2 enzymes.

The structures of the known compounds are shown in (**Figure 1**) and were identified as malabaricones A - C, E (**1** - **3**,**4**)[13,14], giganteone A (**5**),[15] pisiferic acid (**6**),[16] O-methyl pisiferic acid (**7**),[17] pisiferal (**8**)[18] pisiferanol (**9**),[19] flavaspidic acid AB (**10**),[20] triflavaspidic acid ABA (**11**),[21] α-linolenic acid (**12**)[22] and betulonic acid (**13**)[23]. All the compounds having similar spectroscopic data with those reported in the literature. Compounds **1**-**3** were the major metabolites in the fruits of *M. cinnamomea*, while the remaining compounds were obtained in smaller amounts in their respective plants.

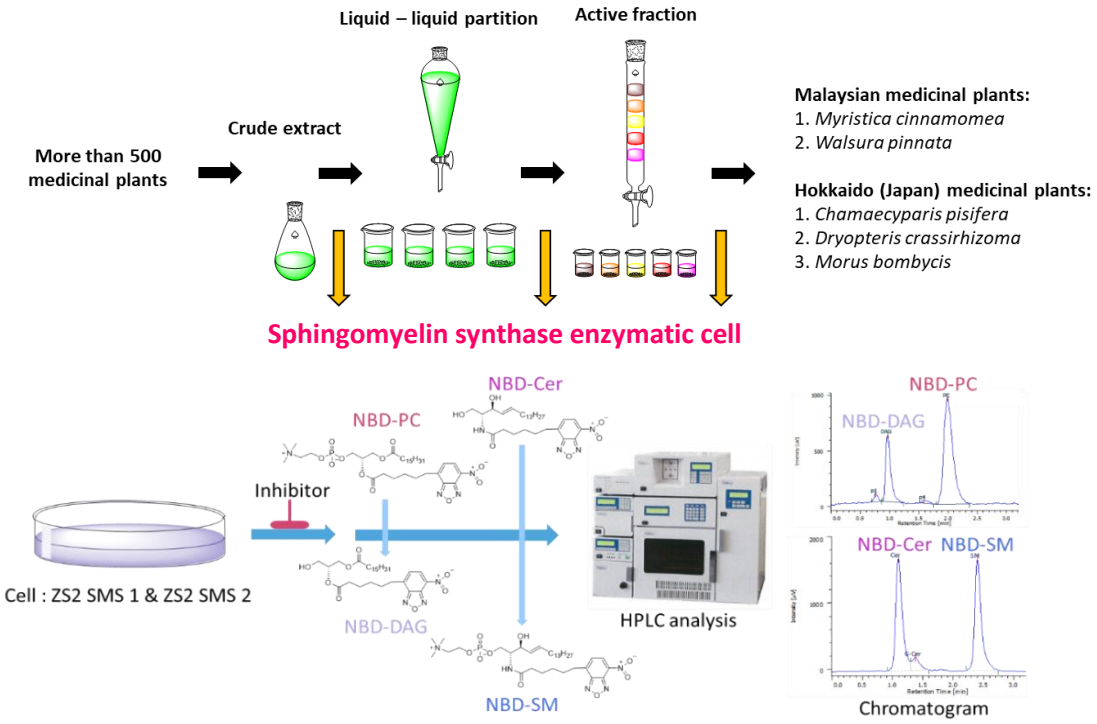

Scheme 1. Screening of plant extracts libraries and assay method development by HPLC.

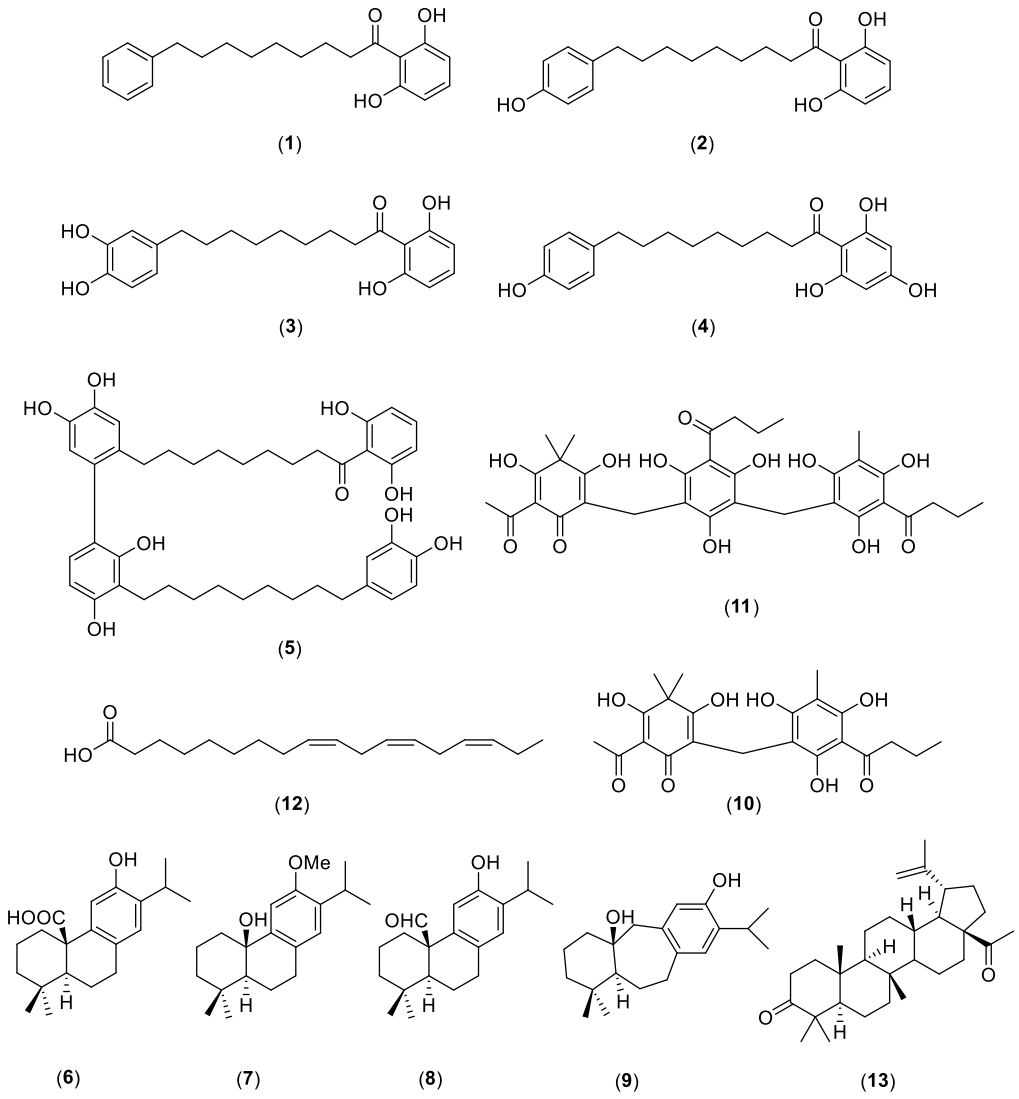

Figure 1. Bioassay-guided of active medicinal plant extracts afforded 13 natural occurring inhibitors for SMS inhibitory activity.

We also employed the sphingomyelin synthase (SMS) assay method development by using high performance liquid chromatography (HPLC) as one of our strategies to facilitates the high throughput screening. This method consists of several procedures which include cell cultures, preparation of cell lysates, reaction and extraction, and analysis using HPLC. Mouse embryonic fibroblast cells which expressed either SMS 1 or SMS2 were culture and cell lysates were prepared and diluted to (protein concentration 0.1 µg/µL). 100 µL of cell lysates were added with 1 µL of inhibitor of various concentration and incubated. As for the reaction, the solutions were added with 1 µL of C6-NBD-ceramide or 1 µL of C6-NBD-phosphocholine and incubated for 3 h at 37°C. The reaction was stopped by addition of Methanol/Chloroform and the mixture was shaken and centrifuged. The formation of C6-NBD-sphingomyelin or C6-NBD-diacylglycerol was quantified by determination of the peak area of C6-NBD-sphingomyelin or C6-NBD-diacylglycerol using HPLC (**Scheme 2**).

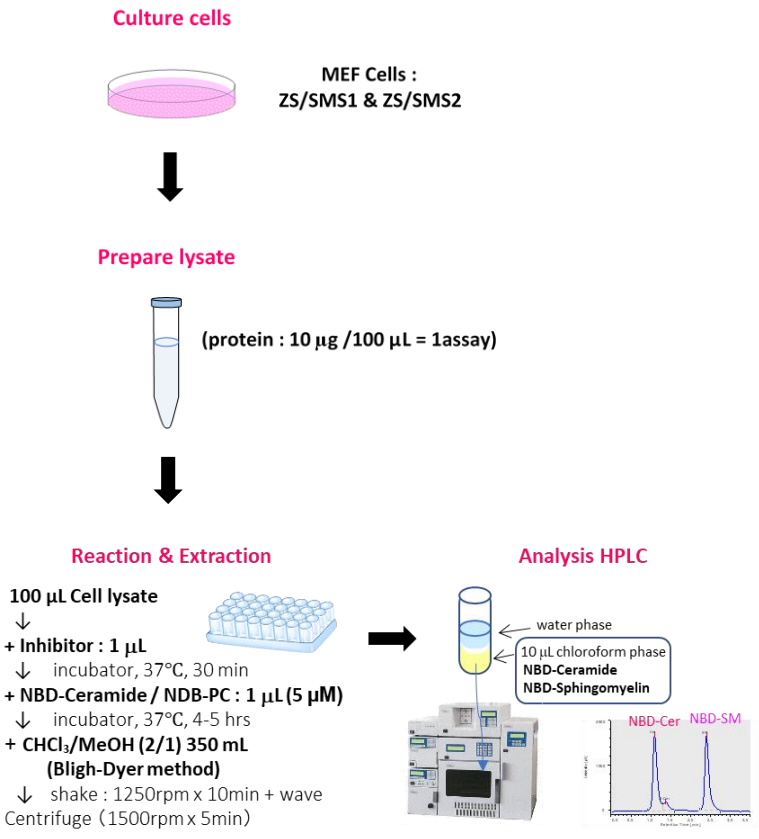

Scheme 2. Sphingomyelin synthase (SMS) enzymatic cell lysate assays.

Subsequently, compounds **1-13** were subjected to SMS inhibition assay by lysate-based assay of SMS1- or SMS2-expressed SMS1/2 double knockout mouse fibroblasts. Each of compounds showed relatively good to moderate inhibition activities against both substrates NBD-ceramide and NBD-phosphocholine (**Table 1**). Herein, we showed that compounds **1** and **3** are the first natural SMS inhibitors identified against both substrates involved in the catalysation reaction.

Table 1. Inhibitory activity of Sphingomyelin synthase (cell lysate).

Compounds		NBD - Cer		NBD - PC	
		SMS 1	SMS 2	SMS 1	SMS 2
No.	Plants	(IC_{50}, µM)	(IC_{50}, µM)	(IC_{50}, µM)	(IC_{50}, µM)
1	*M. Cinnamomea*	4	4	40	50
2	*M. Cinnamomea*	3.5	2.5	-	-
3	*M. Cinnamomea*	3	1.5	20	10
4	*M. Cinnamomea*	6	4.5	-	-
5	*M. Cinnamomea*	15	10	-	-
6	*C. pisifera var filifera*	30	35	-	100
7	*C. pisifera var filifera*	5	20	90	50
8	*C. pisifera var filifera*	3	35	-	90
9	*C. pisifera var filifera*	4	40	100	-
10	*D. crassirhizoma*	10	30	-	-
11	*D. crassirhizoma*	2	3.5	-	-
12	*M. bombycis*	18	23	-	-
13	*W. pinnata*	4.5	>100	100	-

IC_{50} values are the means of three separate determinations on SMS1 or SMS2 expressed SMS1/2 double knockout mouse fibroblast cell lysate and were determined by more than four concentrations of each inhibitor.

Considering the facts that we afforded an α-linolenic acid from the previous screening results, it inspired us to screen a series of fatty acids which composed of unsaturated and saturated fatty acid against SMS inhibitory activity in an effort to introduce promising functional food properties. As a result, docosahexaenoic acid (DHA), eicosapentaenoic acid (EPA) and arachidonic acid (AA) showed better inhibition of SMS1 in an IC_{50} of 3, 4, 4 µM respectively. While erucic acid, docosahexaenoic acid (DHA) and eicosapentaenoic acid (EPA) exhibited an IC_{50} of 8, 15, 16 µM respectively for SMS2 (**Figure 2**). These results demonstrate that unsaturated fatty acid particularly omega-3 displaying stronger inhibition compared to saturated fatty acids. This could be associated with the previously reported study which suggests that omega-3 fatty acids reduce blood triglyceride levels, lower blood pressure and increase insulin sensitivity[24]. Further study needs to be done in order to confirm the specific inhibition by selected free fatty acids.

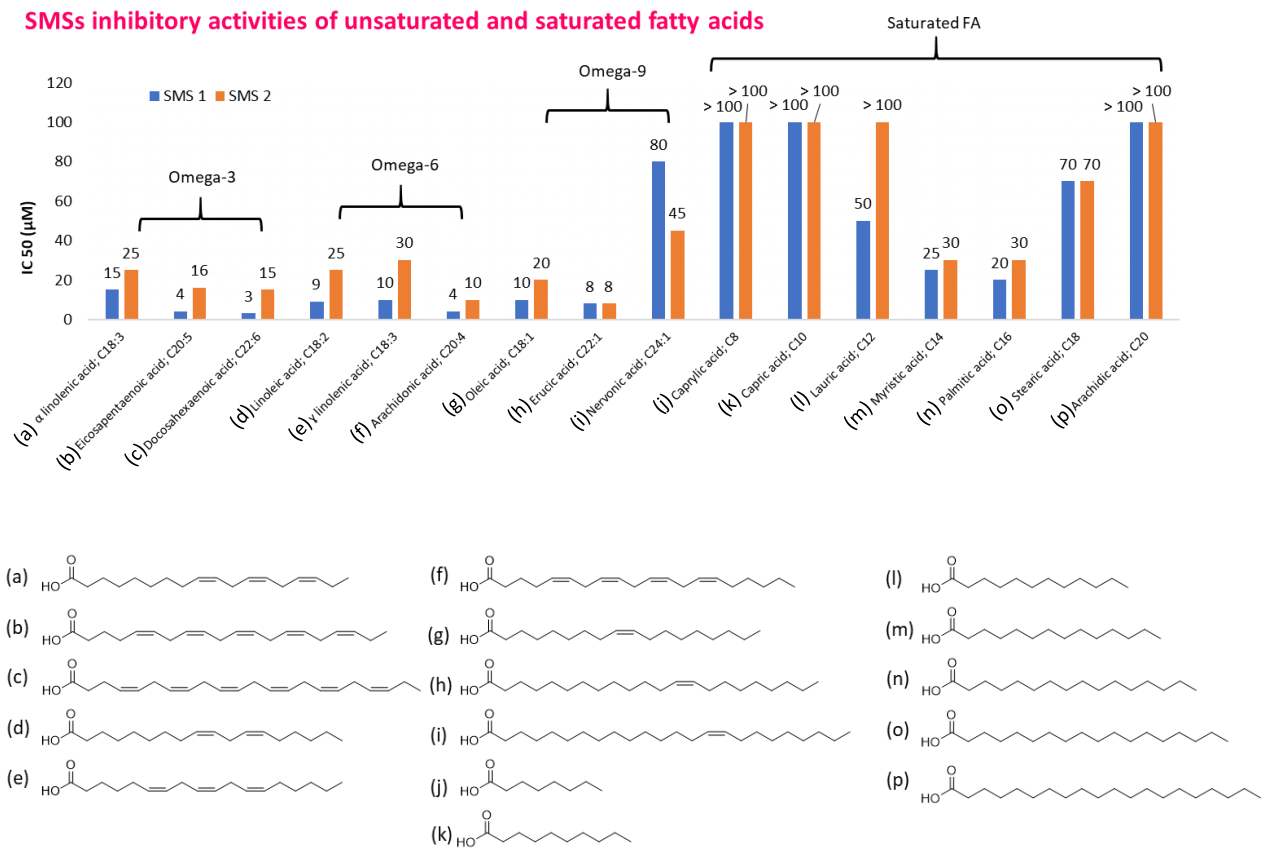

Figure 2. Screening results of saturated and unsaturated free fatty acids against SMSs enzymes.

Conclusion

In summary, 13 natural occurring SMS inhibitors were identified from our medicinal plant extracts library screening assays by using both fluorescence substrates (NBD-ceramide and NBD-phosphocholine). Although the inhibition of the fatty acids could be an initial step to study the enzymes specificity, further investigation needs to be done since it involves the membrane protein which carried out almost all of the chemical reactions that happens in the cells. In the next chapter, we are focusing only for the investigation of potential SMS inhibitors from the fruits of *M. cinnamomea*. It is due to the facts that they exhibit good inhibitory activities of SMS as compared with the rest of the compounds while some of them exists as major compounds.

2.4 Experimental Section

General experimental method

All chemicals and solvents were obtained from commercial supplier and used without further purification. ^{1}H NMR (500 MHz) and ^{13}C NMR (125 MHz) spectra were recorded on a Varian Inova instrument at 25 °C in $CDCl_3$ and CD_3OD purchased from Cambridge Isotope Laboratories, Inc. (Tewksbury, USA). Chemical shifts (δ) are reported in ppm and coupling constant values (*J*) are in hertz relative to $CDCl_3$ (^{1}H, δ 7.26; ^{13}C, δ 77.00) or CD_3OD (^{1}H, δ 3.4, 4.8; ^{13}C, δ 49.3) and tetramethylsilane. The following abbreviations were used for signal multiplicities: s = singlet; d = doublet; t = triplet; q = quartet; p = pentet and m = multiplet. High Resolution Mass spectra (HRMS (ESI)) were obtained from AB sciex Triple TOF® 5600+ at Platform for Research on Biofunctional Molecules, Hokkaido University. Low-resolution mass spectra (ESI-MS) were obtained by a JEOL JMS-T100LP spectrometer. Analytical TLC was performed on 0.2 mm silica gel plates (Merck 60 F-254). SiO_2 gel column chromatography was carried out using silica gel (Wakogel® N60, spherical, 38-100 μm) with air flashing. The purity of isolated compounds was determined by NMR, all the compounds have purity of >90-95%.

Plants material

Myristica cinnamomea King and *Walsura pinnata* Husks were collected from Malaysia. The plants were identified by Mr. Teo Leong Eng and voucher specimens were deposited at the University of Malaya herbarium. While *Chamaecyparis pisifera var filifera*, *Dryopteris crassirhizoma*, *Morus bombycis* were collected inside Hokkaido University, Japan and all the sample specimens were deposited in the laboratory of molecular chemical biology.

Isolation of active compounds from the active extracts

Screening results showed only 5 extracts were identified with good inhibition against target enzymes which were *M. cinnamomea, C. var filifera, D. crassirhizoma, M. bombycis* and *W. pinnata*. The bioassay guided fractionation of the active medicinal plant extracts resulted in the isolation of malabaricones A-C (**1-3**)[13], malabaricone E (**4**)[14], giganteone A (**5**),[15] pisiferic acid (**6**),[16] O-methyl pisiferic acid (**7**),[17] pisiferal (**8**)[18] pisiferanol (**9**),[19] flavaspidic acid AB (**10**),[20] triflavaspidic acid ABA (**11**),[21] α-linolenic acid (**12**)[22] and betulonic acid (**13**)[23]. All the compounds having similar spectroscopic data with those reported in the literature. All isolated known compounds were confirmed by NMR spectroscopy, ESI-MS and having similar spectroscopic data with those reported in the literatures.

Malabaricone A (**1**) was obtained as a pale yellow, amorphous powder; HRMS (*m/z*): $[M + H]^+$, calculated for $C_{21}H_{27}O_3$: 327.1954; found : 327.1950. ^{1}H NMR (MeOH-d_4, 500 MHz): δ = 7.21 (2H, m), 7.18 (1H, t, J = 8.2 Hz), 7.15 (3H, m), 6.34 (2H, d, J = 8.2 Hz), 3.10 (2H, t, J = 7.3 Hz), 2.58 (2H, t, J = 7.3 Hz), 1.66 (2H, p, J = 7.3 Hz), 1.59 (2H, p, J = 7.3 Hz), 1.33 (8H, br s). ^{13}C NMR (MeOH-d_4, 125 MHz): δ = 209.8, 163.6, 163.6, 144.1, 137.0, 129.5, 129.5, 129.4, 129.4, 126.7, 111.5, 108.5, 108.5, 45.9, 37.1, 32.9, 30.8, 30.7, 30.6, 30.4, 25.9.

Malabaricone B (**2**) was obtained as a pale yellow, amorphous powder; HRMS (*m/z*): $[M + H]^+$, calculated for $C_{21}H_{27}O_4$: 343.1903; found : 343.1903. ^{1}H NMR (MeOH-d_4, 500 MHz): δ = 7.19 (1H, d, J =8.2 Hz), 6.97 (2H, d, J = 8.2 Hz), 6.67 (2H, d, J = 8.2 Hz), 6.33 (2H, d, J = 8.2 Hz), 3.11 (2H, t, J = 7.3 Hz), 2.49 (2H, t, J = 7.3 Hz), 1.67 (2H, p, J = 7.3 Hz), 1.55 (2H, p, J = 7.3 Hz), 1.34 (8H, br s). ^{13}C NMR (MeOH-d_4, 125 MHz): δ = 209.8, 163.6, 163.6, 144.1, 137.0, 129.5, 129.5, 129.4, 129.4, 126.7, 111.5, 108.5, 108.5, 45.9, 37.1, 32.9, 30.8, 30.7, 30.6, 30.4, 25.9.

Malabaricone C (**3**) was obtained as a yellow, amorphous powder; HRMS (*m/z*): $[M + H]^+$, calculated for $C_{21}H_{27}O_5$: 359.1853; found : 359.1862. ^{1}H NMR (MeOH-d_4, 500 MHz): δ = 7.19 (1H, d, J = 8.2 Hz), 6.65 (1H, d, J = 8.2 Hz), 6.60 (1H, d, J = 2.0 Hz), 6.47 (1H, dd, J = 8.2, 2.0 Hz), 6.34 (2H, d, J = 8.2 Hz), 3.11 (2H, t, J = 7.3 Hz), 2.44 (2H, t, J = 7.3 Hz), 1.67 (2H, p, J = 7.3 Hz), 1.54 (2H, p, J = 7.3 Hz), 1.33 (8H, br s). ^{13}C NMR (MeOH-d_4, 125 MHz): δ = 209.8, 163.6, 163.6, 146.1, 144.2, 137.0, 135.9, 120.8, 116.6, 116.3, 111.5, 108.5, 108.5, 45.9, 36.4, 33.1, 30.8, 30.7, 30.7, 30.4, 25.9.

Malabaricone E (**4**) was obtained as a yellow, amorphous powder; HRMS (*m/z*): $[M + H]^+$, calculated for $C_{21}H_{27}O_5$: 359.1853; found : 359.1861. ^1H NMR (MeOH-d_4, 400 MHz): δ = 6.97 (2H, d, J = 8.0 Hz), 6.67 (2H, d, J = 8.0 Hz), 5.80 (2H, s), 3.02 (2H, t, J = 8.0 Hz), 2.49 (2H, t, J = 8.0 Hz), 1.65 (2H, p, J = 8.0 Hz), 1.56 (2H, br t, J = 8.0 Hz), 1.33 (8H, br s). ^{13}C NMR (MeOH-d_4, 100 MHz): δ = 206.1, 164.6, 164.4, 164.4, 154.8, 133.5, 128.8, 128.8, 114.5, 114.5, 103.9, 94.3, 94.3, 43.4, 34.6, 31.6, 29.2, 29.2, 29.1, 28.9, 24.8.

Giganteone A (**5**) was obtained as brown viscous oil; ESI-Mass (*m/z*): 715.3427 $[M+H]^+$, 737.3241 $[M+Na]^+$ Molecular formula: $C_{42}H_{50}O_{10}$. ^1H NMR (MeOH-d_4, 500 MHz): δ = 7.18 (1H, t, J = 8.2 Hz), 7.05 (1H, d, J = 8.2 Hz), 6.68 (1H, s), 6.64 (1H, d, J = 8.2 Hz), 6.59 (1H, d, J = 2.0 Hz), 6.53 (1H, s), 6.46 (1H, dd, J = 8.2, 2.0 Hz), 6.41 (1H, d, J = 8.2 Hz), 6.33 (1H, d, J = 8.2 Hz), 3.14 (2H, t, J = 7.3 Hz), 3.08 (2H, t, J = 7.3 Hz), 2.42 (2H, t, J = 7.3 Hz), 2.29 (2H, t, J = 7.3 Hz), 1.67 (2H, m), 1.60 (2H, m), 1.52 (2H, m), 1.30 (18H, brs)

Pisiferic acid (**6**) was obtained as a light yellow, amorphous powder; ESI-Mass (*m/z*): 339.1854 $[M + Na]^+$, Molecular formula: $C_{20}H_{28}O_3$. ^1H NMR (CD_3OD-d_4, 500 MHz): δ = 0.83 (3H, s), 0.96 (3H, s), 1.18 (6H, d, J = 6.8 Hz), 3.19(1H, sep, J =6.8Hz), 6.72 (lH, s), 6.83 (1H, s)

O-methyl pisiferic acid (**7**) was obtained as light yellow, amorphous powder; ESI-Mass (*m/z*): 353.1924 $[M + Na]^+$, Molecular formula: $C_{21}H_{30}O_3$. ^1H NMR (MeOH-d_4, 500 MHz): δ = 0.85 (3H, s), 1.00 (3H, s), 1.21 (6H, d, J=6.8 Hz), 3.19 (1H, sep, J=6.8 Hz), 3.76 (3H, s), 6.78 (1H, s), 6.94 (1H, s)

Pisiferal (**8**) was obtained as light yellow, amorphous powder; ESI-Mass (*m/z*): 323.1883 $[M + Na]^+$, Molecular formula: $C_{20}H_{28}O_2$. ^1H NMR (MeOH-d_4, 400 MHz): δ = 0.85 (3H, s), 1.03 (3H, s), 1.26 (1H, m), 1.23 and 1.23 (each 3H, d, J = 7 Hz), 1.29 (1H, m), 1.50 (1H, dt, J = 13 and 3.5 Hz), 1.70 (3H, m), 2.07 (2H, m), 2.95 (1H, dt, J = 12.6 and 3.7 Hz), 2.99 (2H, m), 3.21 (1H, quint, J = 7 Hz), 6.75 (1H, s), 6.94 (1H, s), 9.91 (1H, s)

Pisiferanol (**9**) was obtained as a light yellow, amorphous powder; ESI-Mass (*m/z*): 301.2320 $[M - H]^-$, Molecular formula: $C_{20}H_{30}O_2$. ^1H NMR (MeOH-d_4, 400 MHz): δ = 0.93 (3H, s), 0.96 (3H, s), 1.22 (3H, d, J = 6.2 Hz), 1.22 (3H, d, J = 6.2 Hz), 2.66 (1H, d, J = 13.9 Hz), 2.71 (1H, d, J = 11.4 Hz,), 2.79 (1H, dd, J = 13.9, 6.2 Hz), 3.09 (1H, d, J = 13.9 Hz), 3.23 (1H, sept, J = 6.6 Hz), 6.80 (1H, s), and 6.93 (1H, s)

Flavaspidic acid AB (**10**) was obtained as a pale yellow amorphous powder; ESI-Mass (*m/z*): 419.5510 $[M + H]^+$, Molecular formula: $C_{22}H_{26}O_8$. ^1H NMR (MeOH-d_4, 500 MHz): δ = 0.99 (3H, t, J = 7.2 Hz), 1.40 (6H, brs), 1.74 (2H, m), 2.12 (3H, s), 2.74 (3H, s), 3.10 (2H, m), 3.57 (2H, brs)

Triflavaspidic acid ABA (**11**) was obtained as a light yellow amorphous powder; ESI-Mass (*m/z*): 625.3033 $[M - H]^-$, Molecular formula: $C_{33}H_{38}O_{12}$. ^1H NMR (MeOH-d_4, 500 MHz): δ = 3.42 (2H, s), 2.52 (3H, s), 1.25 (3H, s), 1.25 (3H, s), 3.53 (2H, brs), 3.06 (2H, m), 1.66 (4H, m), 0.98 (6H, m), 1.93 (3H, s), 3.06 (2H, m)

α -linolenic acid (**12**) was obtained as a light yellow oil; ESI-Mass (*m/z*): 277.1022 $[M - H]^-$, Molecular formula: $C_{18}H_{30}O_2$. ^1H NMR ($CDCI_3$-*d*, 500 MHz): δ = 5.37 (6H, m), 2.82 (4H, t, J = 8.2 Hz), 2.35 (2H, m), 2.68 (4H, m), 1.64 (2H, m), 1.30 (8H, brs), 0.98 (3H, t, J = 8.2 Hz)

Betulonic acid (**13**) was obtained as a white, amorphous powder; ESI-Mass (*m/z*): 455.123 $[M + H]^+$, Molecular formula: $C_{30}H_{46}O_3$. ^1H NMR ($CDCI_3$-*d*, 400 MHz): δ = 4.68 (1H, s), 4.55 (1H, s), 3.24 (1 H, t), 2.99 (1H, dd), 2.23 (1H, m), 1.65 (3H, s), 1.02–1.95 (3H, m), 1.02 (3H, s), 1.00 (3H, s), 0.98 (3H, s), 0.86 (3H, s), 0.85 (3H, s).

Cell culture

The mouse embryonic fibroblast (tMEF) containing ZS/SMS1 and ZS/SMS2, WT-tMEF were p resented from Prof. Igarashi (Lipid Bio Section, Faculty of Advanced Life Science, Hokkaido University). ZS cells was isolated from a SMS1, SMS2 double KO MEF, which was immortalized using SV40T antigen. ZS cells stably expressed SMS1 or SMS2, were named ZS/SMS1 and ZS/SMS2.[5] HepG2 cells were obtained from ATCC. Cells were cultured in dulbecco's modified eagle's medium (DMEM) supplemented with 10% (v/v) fetal bovine serum (FBS), 1% (v/v) penicillin with streptomycin at 34 °C in a 5% CO_2 incubator.

Measurement of SMSs inhibitory activity in cell lysates

Cell lysates were prepared as follows: ZS/SMS1 and ZS/SMS2 cells (protein concentration 0.1 µg/µL) were diluted by 20 mM Tris-buffer (pH 7.5) and sonicated. Aliquots of the cell lysates 100 µL were added with 1 µL of inhibitor of desired concentration and incubated at 37°C. After 30 min, the solutions were added with 1 µL of C6-NBD-ceramide (5 µM), and incubated for 3 h at 37°C. The reaction was stopped by addition of 400 µL of Methanol/Chloroform [1/2 (v/v)]; the mixture was shaken and centrifuged (1500 rpm x 5 min). The formation of C6-NBD-sphingomyelin was quantified by determination of the peak area of C6-NBD-sphingomyelin using high performance liquid chromatography (HPLC). A reverse phase HPLC assay using a JACSO HPLC system was developed for the quantitative analysis of the inhibitory activity. The system was equipped with a PU-2089 Plus and FP-2020 Plus set at λex = 470 nm and λem = 530 nm. A 50 x 4.6 YMC-Pack Diol-120-NP column (5-µm particle size) was used with mobile phase (IPA/hexane/water) at a flow rate of 1.0 mL/min.[25]

2.5 References

(1) Ullman, M. D.; Radin, N. S. The Enzymatic Formation of Sphingomyelin from Ceramide and Lecithin in Mouse Liver. *J. Biol. Chem.* **1974**, *249* (5), 1506–1512.

(2) Merrill, A. H.; Jones, D. D. An Update of the Enzymology and Regulation of Sphingomyelin Metabolism. *Biochim. Biophys. Acta - Lipids Lipid Metab.* **1990**, *1044* (1), 1–12.

(3) Bienias, K.; Fiedorowicz, A.; Sadowska, A.; Prokopiuk, S.; Car, H. Regulation of Sphingomyelin Metabolism. *Pharmacol. Reports* **2016**, *68* (3), 570–581.

(4) Hannun, Y. A. Functions of Ceramide in Coordinating Cellular Responses to Stress. *Science* **1996**, *274* (5294), 1855–1859.

(5) Mitsutake, S.; Zama, K.; Yokota, H.; Yoshida, T.; Tanaka, M.; Mitsui, M.; Ikawa, M.; Okabe, M.; Tanaka, Y.; Yamashita, T.; et al. Dynamic Modification of Sphingomyelin in Lipid Microdomains Controls Development of Obesity, Fatty Liver, and Type 2 Diabetes. *J. Biol. Chem.* **2011**, *286* (32), 28544–28555.

(6) Yuyama, K.; Sun, H.; Mitsutake, S.; Igarashi, Y. Sphingolipid-Modulated Exosome Secretion Promotes Clearance of Amyloid-β by Microglia. *J. Biol. Chem.* **2012**, *287* (14), 10977–10989.

(7) Hanamatsu, H.; Ohnishi, S.; Sakai, S.; Yuyama, K.; Mitsutake, S.; Takeda, H.; Hashino, S.; Igarashi, Y. Altered Levels of Serum Sphingomyelin and Ceramide Containing Distinct Acyl Chains in Young Obese Adults. *Nutr. Diabetes* **2014**, *4* (10), e141.

(8) Kim, Y.-J.; Greimel, P.; Hirabayashi, Y. GPRC5B-Mediated Sphingomyelin Synthase 2 Phosphorylation Plays a Critical Role in Insulin Resistance. *iScience* **2018**, *8*, 250–266.

(9) Yuyama, K.; Mitsutake, S.; Igarashi, Y. Pathological Roles of Ceramide and Its Metabolites in Metabolic Syndrome and Alzheimer's Disease. *Biochim. Biophys. Acta - Mol. Cell Biol. Lipids* **2014**, *1841* (5), 793–798.

(10) Ohnishi, T.; Hashizume, C.; Taniguchi, M.; Furumoto, H.; Han, J.; Gao, R.; Kinami, S.; Kosaka, T.; Okazaki, T. Sphingomyelin Synthase 2 Deficiency Inhibits the Induction of Murine Colitis-Associated Colon Cancer. *FASEB J.* **2017**, *31* (9), 3816–3830.

(11) Fan, Y.; Shi, F.; Liu, J.; Dong, J.; Bui, H. H.; Peake, D. A.; Kuo, M.-S.; Cao, G.; Jiang, X.-C. Selective Reduction in the Sphingomyelin Content of Atherogenic Lipoproteins Inhibits Their Retention in Murine Aortas and the Subsequent Development of Atherosclerosis. *Arterioscler. Thromb. Vasc. Biol.* **2010**, *30* (11), 2114–2120.

(12) Swamy, M. M. M.; Murai, Y.; Ohno, Y.; Jojima, K.; Kihara, A.; Mitsutake, S.; Igarashi, Y.; Yu, J.; Yao, M.; Suga, Y.; et al. Structure-Inspired Design of a Sphingolipid Mimic Sphingosine-1-Phosphate Receptor Agonist from a Naturally Occurring Sphingomyelin Synthase Inhibitor. *Chem. Commun.* **2018**, *54* (90), 12758–12761.

(13) Purushothaman, K. K.; Sarada, A.; Connolly, J. D. Malabaricones A–D, Novel Diarylnonanoids from Myristica Malabarica Lam (Myristicaceae). *J. Chem. Soc.*,

Perkin Trans. 1 **1977**, *0* (5), 587–588.

(14) Abdul Wahab, S. M.; Sivasothy, Y.; Liew, S. Y.; Litaudon, M.; Mohamad, J.; Awang, K. Natural Cholinesterase Inhibitors from Myristica Cinnamomea King. *Bioorg. Med. Chem. Lett.* **2016**, *26* (15), 3785–3792.

(15) Pham, V. C.; Jossang, A.; Sévenet, T.; Bodo, B. Novel Cytotoxic Acylphenol Dimers of Myristica Gigantea; Enzymatic Synthesis of Giganteones A and B. *Tetrahedron* **2002**, *58* (28), 5709–5714.

(16) Fukui, H.; Koshimizu, K.; Egawa, H. A New Diterpene with Antimicrobial Activity from *Chamaecyparis Pisifera* Endle. *Agric. Biol. Chem.* **1978**, *42* (7), 1419–1423.

(17) Kobayashi, K.; Nishino, C. *Biological Activities of Pisiferic Acid and O-Methyl-Pisiferic Acid*; 1986; Vol. 50.

(18) Fraga, B. M.; Díaz, C. E.; Guadaño, A.; González-Coloma, A. Diterpenes from Salvia Broussonetii Transformed Roots and Their Insecticidal Activity. *J. Agric. Food Chem.* **2005**, *53* (13), 5200–5206.

(19) Hasegawa, S.; Kojima, T.; Hirose, Y. Terpenoids from the Seed of Chamaecyparis Pisifera: The Structures of Six Diterpenoids. *Phytochemistry* **1985**, *24* (7), 1545–1551.

(20) Ren, Q.; Quan, X.; Wang, Y.; Wang, H. Isolation and Identification of Phloroglucinol Derivatives from Dryopteris Crassirhizoma by HPLC-LTQ-Orbitrap Mass Spectrometry. *Chem. Nat. Compd.* **2016**, *52* (6), 1137–1140.

(21) Gao, Z.; Ali, Z.; Zhao, J.; Qiao, L.; Lei, H.; Lu, Y.; Khan, I. A. Phytochemical Investigation of the Rhizomes of Dryopteris Crassirhizoma. *Phytochem. Lett.* **2008**, *1* (4), 188–190.

(22) Yang, Q.; Cao, W.; Zhou, X.; Cao, W.; Xie, Y.; Wang, S. Anti-Thrombotic Effects of α-Linolenic Acid Isolated from Zanthoxylum Bungeanum Maxim Seeds. *BMC Complement. Altern. Med.* **2014**, *14*, 348.

(23) Leong, K. H.; Mahdzir, M. A.; Din, M. F. M.; Awang, K.; Tanaka, Y.; Kulkeaw, K.; Ishitani, T.; Sugiyama, D. Induction of Intrinsic Apoptosis in Leukaemia Stem Cells and in Vivo Zebrafish Model by Betulonic Acid Isolated from Walsura Pinnata Hassk (Meliaceae). *Phytomedicine* **2017**, *26*, 11–21.

(24) Juárez-López, C.; Klünder-Klünder, M.; Madrigal-Azcárate, A.; Flores-Huerta, S. Omega-3 Polyunsaturated Fatty Acids Reduce Insulin Resistance and Triglycerides in Obese Children and Adolescents. *Pediatr. Diabetes* **2013**, *14* (5), 377–383.

(25) Swamy, M. M. M.; Murai, Y.; Ohno, Y.; Jojima, K.; Kihara, A.; Mitsutake, S.; Igarashi, Y.; Yu, J.; Yao, M.; Suga, Y.; et al. Structure-Inspired Design of a Sphingolipid Mimic Sphingosine-1-Phosphate Receptor Agonist from a Naturally Occurring Sphingomyelin Synthase Inhibitor. *Chem. Commun.* **2018**, *54* (90), 12758–12761.

Chapter 3

Malabaricone C as natural sphingomyelin synthase inhibitor against diet-induced obesity and its lipid metabolism in mice

3.1 Abstract

The interaction between natural occurring inhibitors and targeted membrane proteins could be an alternative medicinal strategy for the treatment of metabolic syndrome, notably, obesity. In this study, we identified malabaricones A-C, E (**1**-**4**) isolated from the fruits of *Myristica cinnamomea* King as natural inhibitors for sphingomyelin synthase (SMS), a membrane protein responsible for sphingolipid biosynthesis. Having the most promising inhibition, oral administration of compound **3** exhibited multiple efficacies in reducing weight gain, improving glucose tolerance and reducing hepatic steatosis in high fat diet-induced obesity mice models. Liver lipid analysis revealed a crucial link between the SMS activities of compound **3** and its lipid metabolism *in vitro* and *in vivo*. The non-toxic nature of compound **3** makes it a suitable candidate in search of drugs which can be employed in the treatment and prevention of obesity.

3.2 Introduction

Worldwide prevalence of obesity has increased substantially over the past 40 years and continues to cause metabolic syndrome which is associated with dyslipidaemia, insulin resistance, cardiovascular diseases and type 2 diabetes mellitus (T2DM).[1,2,3] These intersecting risks are controlled by a critical and complex metabolic pathway which involves the membrane protein. Having said that, the membrane protein could be the initial key in enhancing the understanding of pharmacology for common metabolic related diseases, notably, obesity. The membrane protein regulates cell communication with their surroundings which is activated by a wide variety of physiological and environmental stimuli including peptides, proteins, small organic molecules, and even ions.[4,5,6] About more than 50% of all known low molecular drugs bind to the membrane protein.[7,8] Thus, discovering an enzyme inhibitor will be a direct approach in developing low molecular drugs.

This study of ours focuses on the sphingomyelin synthase (SMS) membrane protein family which consists of two isozymes, SMS1 and SMS2.[9,10] Both SMS 1 and 2, catalyze ceramide and phosphatidylcholine (PC) as substrates to produce sphingomyelin (SM) and diacylglycerol (DAG).[11,12] The SMSs modulate SM and other sphingolipids levels, thereby regulating membrane fluidity, ceramide-dependent apoptosis, lipid metabolism and signal transduction.[13,14,15,16] The increasing levels of SM and DAG produced by the SMSs will lead to obesity and insulin resistance.[17,18] SMS knockout mice are resistant to Alzheimer's disease, tumorigenesis, diet-induced obesity, T2DM and are also know to exhibit decreased levels of plasma inflammatory cytokines.[19,20,15,21] Therefore, the inhibition of the SMSs enzymes by natural occurring substrates would be an ideal therapeutic approach for metabolic syndrome.

Very recently, the inhibitory activity of gingkolic acid from the leaves of *Gingko biloba* was reported by our group.[22] Though, gingkolic acid has been proven to be an effective inhibitor with equal inhibiting potentials (IC_{50} = 1.5 µM) against both enzymes, studies have revealed that gingkolic acid is toxic, thus making it an unsuitable candidate for the further development of it as a drug.[23,24] With regard to this, in the present work, we report the isolation of malabaricones A-C, E (**1**-**4**) as the first naturally occurring SMS inhibitors from the edible plants in an effort to display a safe and lesser side effects.[25] Additionally, we performed a diet-induced obesity test with malabaricone C (**3**) that showed significantly preventing high fat diet-induced fatty liver.

3.3 Results and discussion

Preliminary screening of the ethyl acetate extract from the fruits of *M. cinnamomea* showed potential inhibitory activity against SMS1 (13 µg/mL) and SMS2 (10 µg/mL), respectively. Therefore, the bioassay-guided fractionation of the extract resulted in the isolation of malabaricones A-C, E (**1-4**) as the active compounds (**Figure 1**).[26,27] Subsequently, compounds **1-4** were subjected to SMS inhibition assay by lysate-based assay of SMS1- or SMS2-expressed SMS1/2 double knockout mouse fibroblasts. Each of compounds showed relatively moderate inhibition activities compared with that of previously synthesized inhibitors (**Table 1**).[22] A closer look at the structures of compounds **1-4** provided further insight as to how the activities of these compounds might have been influenced by the chemical groups in their respective structures (**Figure 1**). The SMS inhibiting potentials of compounds **1-3** could have enhanced with the increase in the number of hydroxyl groups in their ring b. The lower SMS inhibiting potentials of compound **4** upon comparison to compound **2** may have resulted from the additional hydroxyl group in its ring a.

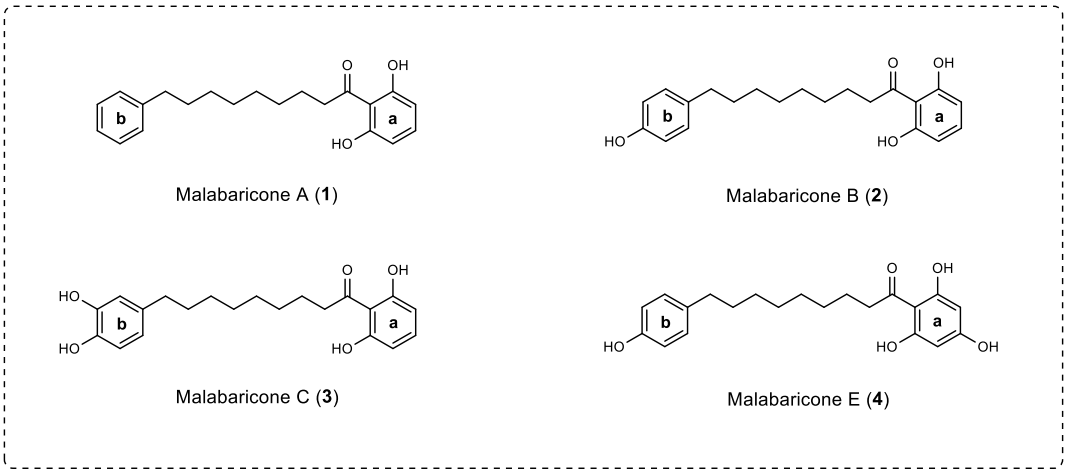

Figure 1. Bioassay-guided of the fruits of *M. cinnamomea* extract afforded 4 natural occurring inhibitors for SMS inhibitory activity.

Table 1. Inhibitory activity of Sphingomyelin synthase (cell lysate).

No.	Compounds	NBD - Ceramide	
		SMS 1	SMS 2
		(IC_{50}, µM)	
1	Malabaricone A	4	4
2	Malabaricone B	3.5	2.5
3	Malabaricone C	3	1.5
4	Malabaricone E	6	4.5

IC_{50} values are the means of three separate determinations on SMS1 or SMS2 expressed SMS1/2 double knockout mouse fibroblast cell lysate and were determined by more than four concentrations of each inhibitor.

To determine the mode of action for major compounds **1-3**, cell lysate assay of the SMS inhibitory activity was carried out by using different substrate concentrations. The IC_{50} values of 2 to 3 µM for SMS1 and 1 to 3 µM for SMS2 were obtained in the presence of 5 and 50 µM of NDB-Ceramide. As a result, changes in substrate concentration did not significantly affect the IC_{50} values of compounds **1-3**, thus, suggesting that compounds **1-3** were non-competitive inhibitor of both SMS 1 and 2 (**Table 2**). Cell counting kit-8 assay was used to evaluate the cytotoxic activity of compound **3** against wild-type mouse embryonic fibroblasts cells, MEF. 56-97 % of the cells were viable after 3 hours of treatment with compound **3** at concentration levels of 1-0.01 mM (**Figure 2A**). Acute toxicity studies of compound **3** at the concentration of 500 mg/kg were previously conducted on mice liver and kidneys (**Figure 2B**). The absent of inflammation, necrosis and haemorrhaging in the respective organs further supported our findings.[28]

Table 2. Mode of inhibition analysis of compounds **1**-**3**.

Compounds	IC_{50}, µM			
	NBD-Ceramide, 5 µM		NBD-Ceramide, 50 µM	
	SMS 1	SMS 2	SMS 1	SMS 2
1	3	3	3	3
2	2	2	2	2.5
3	2.5	1.5	2	1

Changes in substrate concentration do not significantly affect the IC_{50} value of compounds **1-3** suggesting that compounds **1-3** is a non-competitive inhibitor of SMS 1 & 2.

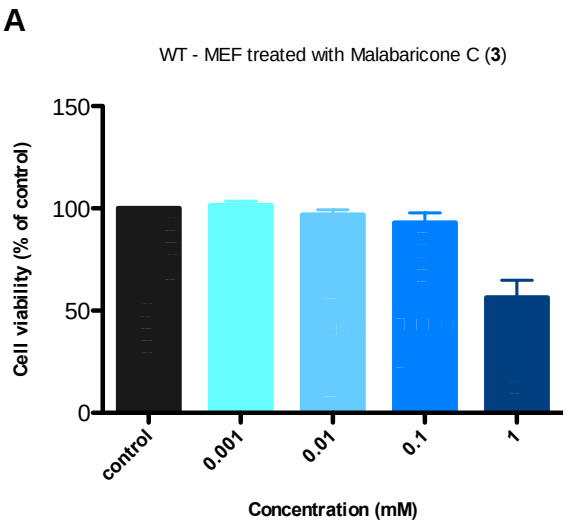

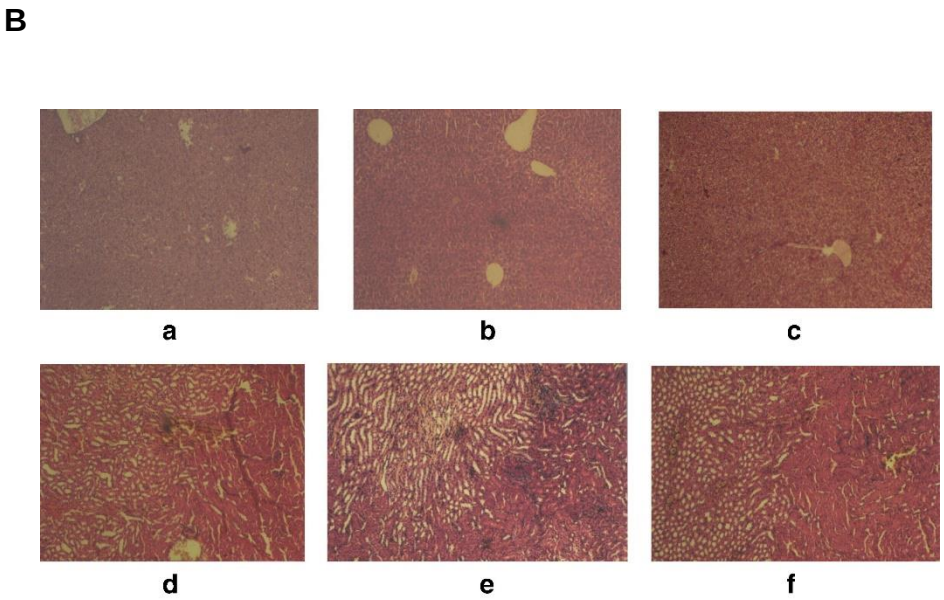

Figures 2. Cytotoxicity analysis. Cell counting kit-8 assay was used to evaluate (A) The cytotoxic activity of compound **3** against wild-type mouse embryonic fibroblasts cells, MEF. Cell viability were analysed after 3 hours of treatment with compound **3** at concentration levels of 1-0.001 mM. Data are presented as the mean ± standard error of the mean (SEM). (B) Previously reported histopathological features of mice liver and kidney following administration of malabaricone B and malabaricone C, each 500 mg/kg body weight per day for 1 month. a–c: livers of normal, malabaricone B-treated and malabaricone C-treated mice; d–f: kidneys of normal, malabaricone B-treated and malabaricone C-treated mice.

Furthermore, in the current investigation, the SMS inhibition assay of compound **3** was carried out with live cells (cell-based assay) and the IC_{50} values were 13 µM and 11 µM for SMS1 and SMS2 enzymes, respectively (**Table 3**). These results suggested that compound **3** could be a suitable candidate for further *in vitro* and *in vivo* studies based on its previously reported world drug index, Lipinski's rules, non-mutagenicity and non-carcinogenicity.[29]

Table 3. The inhibitory activity of Sphingomyelin synthase (cell assay).

Compound	(IC_{50}, µM)	
	SMS 1	SMS 2
3	13	11

IC_{50} values are the means of three separate determinations on SMS1 or SMS2 expressed SMS1/2 double knockout mouse fibroblast cell lysate and were determined by more than four concentrations of each inhibitor.

It has been reported that high fat diet (HFD) activates the nuclear receptor PPAR-ɤ, which is responsible for the hyper-expression of CD36/FAT.[15] The SMS2 enzyme facilitates CD36/FAT to take up the PPAR-ɤ ligands which leads to the accumulation of triglycerides and lipid droplets, thus resulting in fatty liver formation. Since compound **3** exhibited SMS1 and SMS2 inhibitory activities, an oleic acid uptake analysis assay with hepatocytoma HepG2 cells was further conducted to examine the levels of intracellular triglycerides and free fatty acids. Compound **3** decreased the levels of intracellular triglycerides in a dose-dependent manner while it exhibited no significant changes in the free fatty acids levels as compared to the control (**Figures 3A-B**). With the promising *in vitro* effects on oleic acid uptake, we performed a Nile red staining assay to examine the effect of compound **3** on lipid droplet formation in the HepG2 cells. Remarkably, compound **3** for the first time, was found to significantly decrease lipid accumulation in a dose-dependent manner (**Figures 3C-D**). These data indicated that compound **3** was able to prevent cellular uptake by CD36/FAT in a dose dependent manner, which is in good agreement with the results of the previous *in vivo* effects of SMS2 knockout mice.[15]

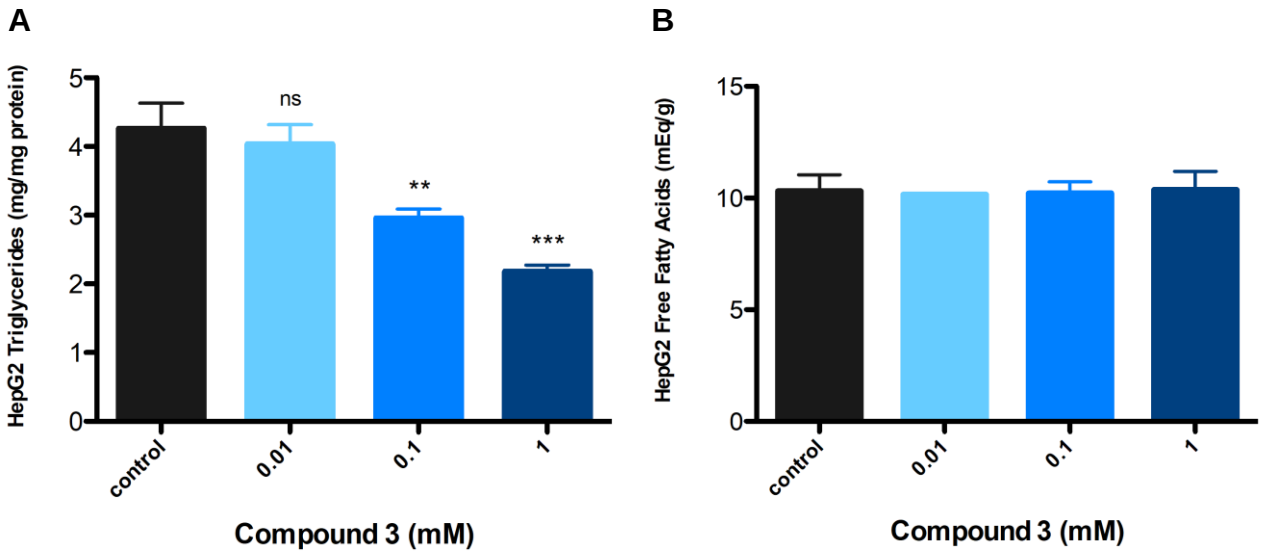
A
HepG2 Triglycerides (mg/mg protein)
5
4
3
2
1
0
ns
**
***
control
0.01
0.1
1
Compound 3 (mM)
B
HepG2 Free Fatty Acids (mEq/g)
15
10
5
0
control
0.01
0.1
1
Compound 3 (mM)

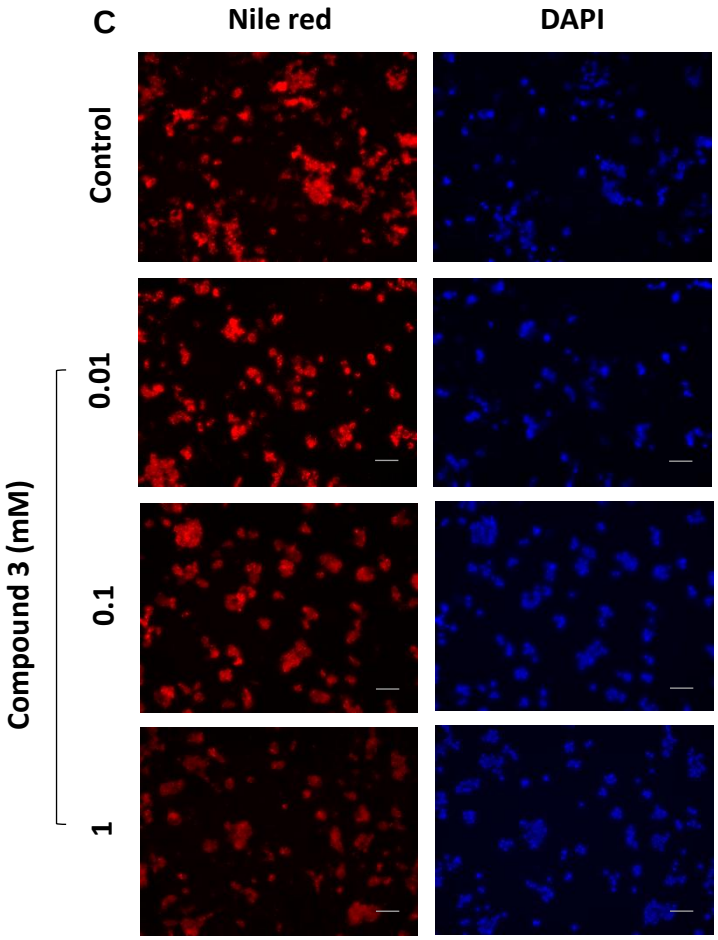
C
Nile red
DAPI
Control
0.01
0.1
1
Compound 3 (mM)

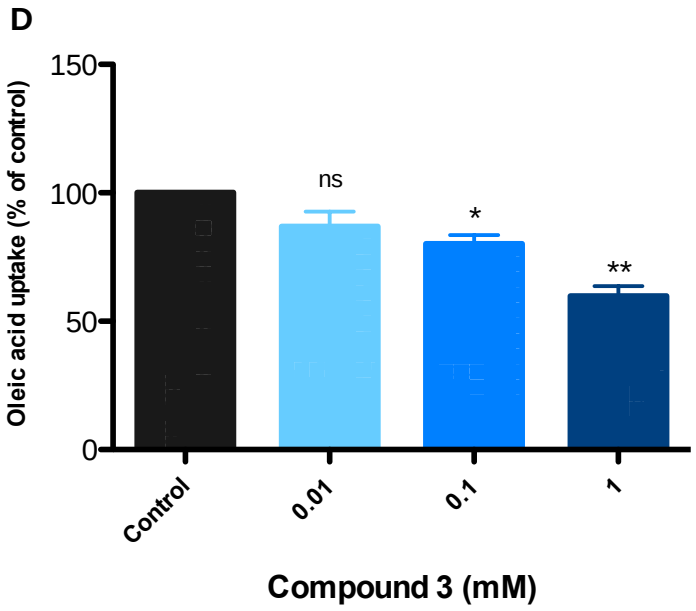

Figure 3. In vitro results of HepG2 cell analysis. Intracellular levels of (A) triglycerides and (B) free fatty acid when treated with different concentration of compound **3** with oleic acid uptake. (C) Representative images of Nile Red staining and DAPI staining. (D) Oleic acid uptake analysis. Lipid droplets were stained with Nile Red and the numbers of lipid droplets were counted using fluorescent microscopy. Scale bar, 100 µm. Data are presented as the mean ± standard error of the mean (SEM); Statistical analysis was done by using t-test: (*) $P < 0.05$, (**) $P < 0.01$, (***) $P < 0.001$, (****) $P < 0.0005$, ns = no significant difference versus the control.

With regard to the *in vitro* results, the selected natural occurring inhibitor was further investigated using (C57BL/6J) mice which were fed with high-fat diet (HFD), normal chow diet (ND) and HFD supplemented with 0.1 % of compound **3**. The HFD + **3** mice were healthy and behaved normally over 2 months with the exception of a noticeably leaner phenotype (**Figure 4A**). Despite of not having any statistically difference in the daily food intake between the HFD control and the HFD + **3** group (**Figure 4B**), the body weight of the HFD + **3** group was significantly lower than those of the controls starting from 20 days of treatment with an inclusive weight loss of 42.7 % (**Figures 4C-D**). In addition, oral glucose tolerance test was performed after 8 weeks of the daily oral administration of the vehicle controls and HFD + **3**.

Treatment of mice with compound **3** also displayed a significant improvement in the glucose tolerance than that of the vehicle-treated mice (**Figure 4E**).

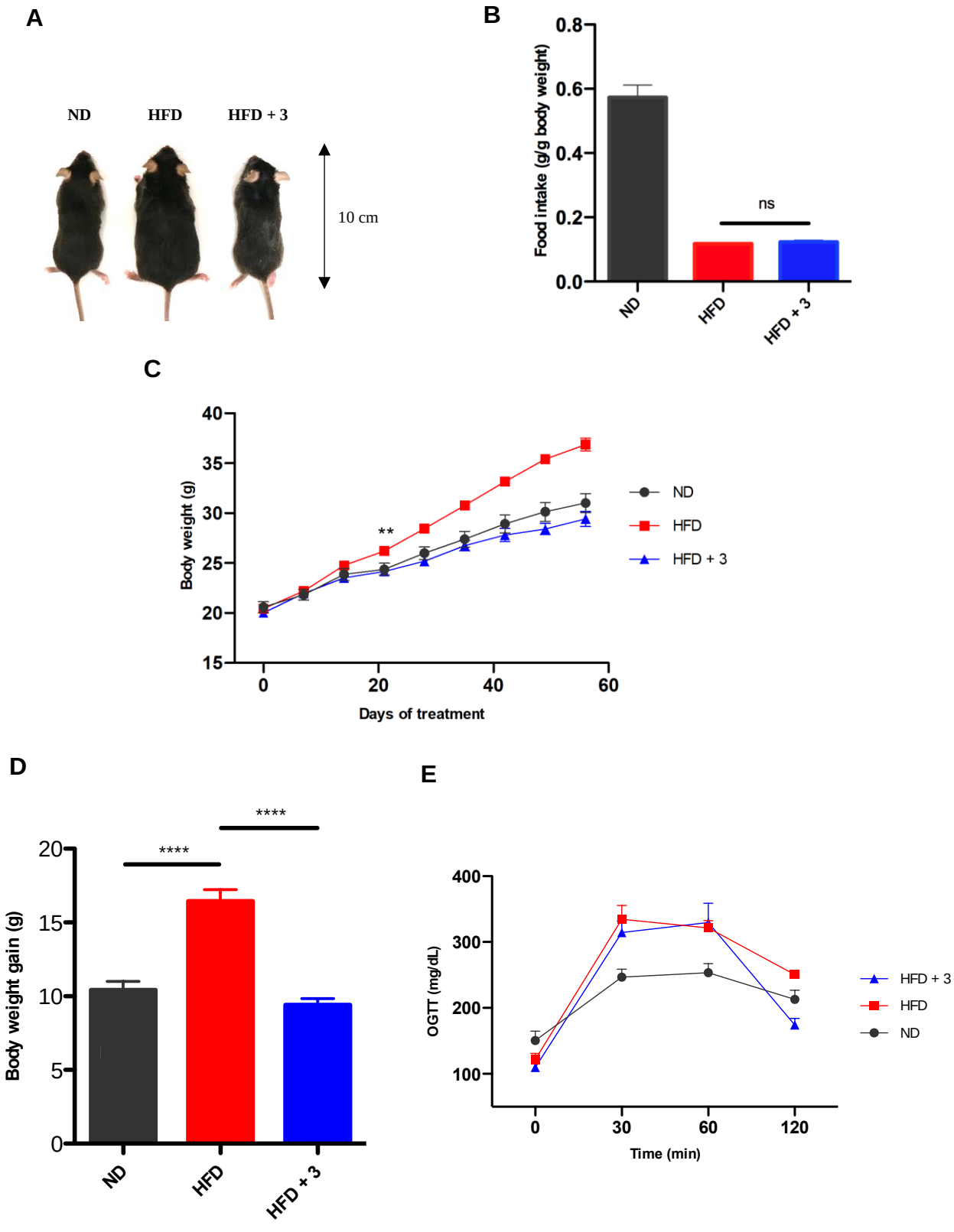

Figure 4. In vivo results of compound **3** on body weight gain and blood glucose levels. (A) Representatives images of the whole mice body; (B) Daily food intake; (C-D) Body weight gain; (E) Oral glucose tolerance test; Control: ND, normal chow diet and HFD, High fat diet; Test group: HFD + **3**, High fat diet with 0.1% of Malabaricone C. Data are presented as mean ± standard error of the mean (SEM); *N* = 7-8 mice per group. Statistical analysis was done by using t-test: (*) $P < 0.05$, (**) $P < 0.01$, (***) $P < 0.001$, (****) $P < 0.0005$, ns = no significant difference versus the control.

The liver plays a key role in lipid metabolism.[30] Liver weight reduction was observed for the HFD + **3** as compared to the HFD group (**Figure 5A**) but the liver of the HFD + **3** group was noticeably redder, possibly implying a decreased fat content in the organ (**Figure 5B**). Previous study has shown that up-regulation of the hepatic lipid metabolism may contribute to the suppression of the liver fat and visceral fat accumulation.[31] Examination of the histological analysis of the oil red O-stained sectioned of the liver tissues showed the presence of numerous steatosis in the HFD control group as indicated by microscopy observation (**Figure 5C**).

The HFD + **3** group on the other hand exhibited resistance in the development of liver steatosis and improved lipid metabolism. Steatosis controls the development of obesity along with metabolic syndrome related disorder.[32] Consistent with the histochemical results, we found that HFD + **3** effectively reduced the hepatic TG levels (**Figure 5D**). In addition, feeding the mice with HFD + **3** significantly reduced the levels of triglycerides (TG) and free fatty acids (FFAs) in the blood plasma (**Figures 5E-F**). In comparison with previous plasma free fatty acids in the SMS2 knockout mice *in vivo*, there is a possibility that the uptake of fatty acids into the liver tissues may not fully be prevented which further explains the decrease of plasma free fatty acids upon feeding with HFD + **3**.

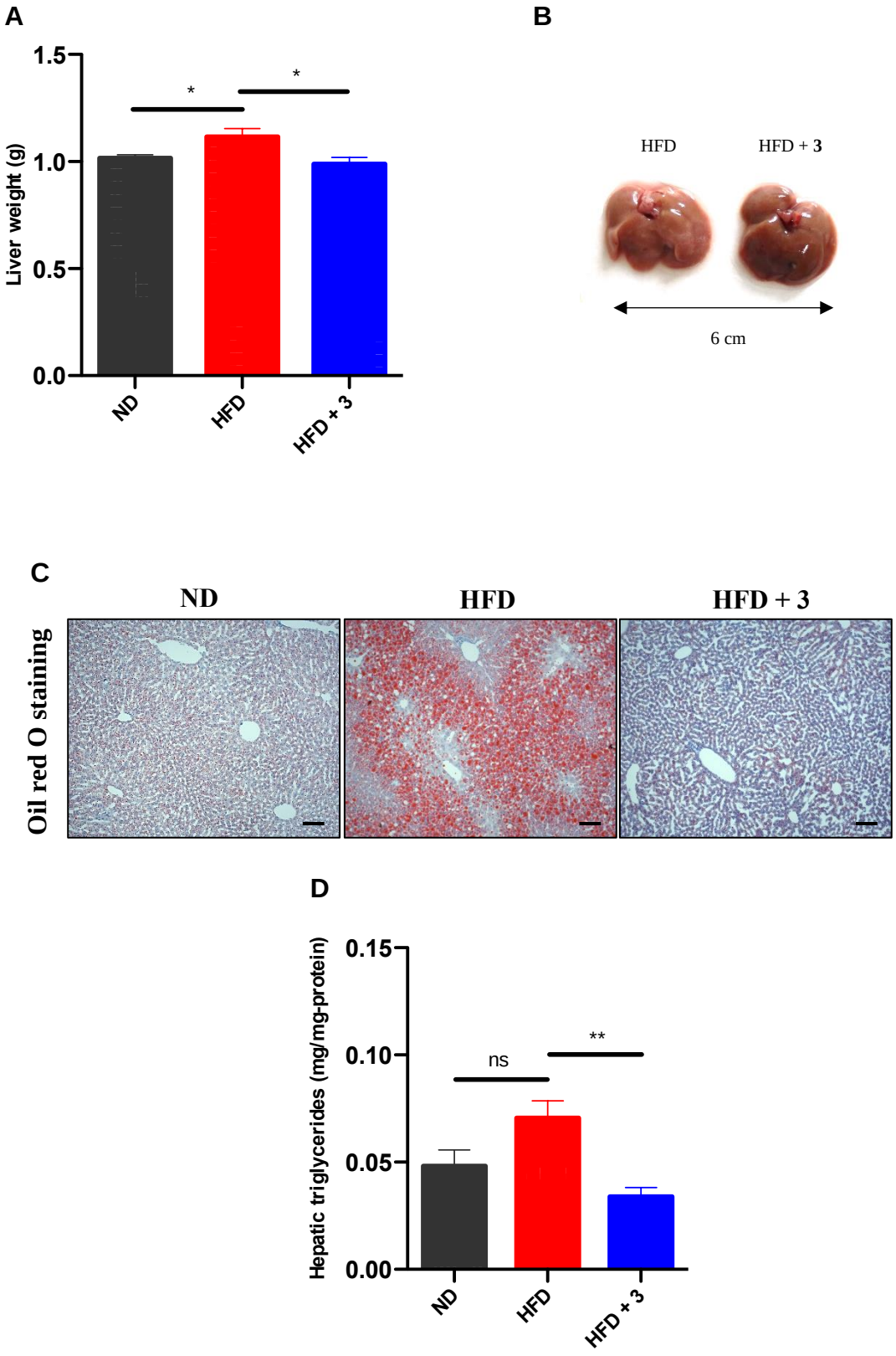
A
Liver weight (g)
1.5
1.0
0.5
0.0
*
*
ND
HFD
HFD + 3
B
HFD
HFD + 3
6 cm
C
ND
HFD
HFD + 3
Oil red O staining
D
Hepatic triglycerides (mg/mg-protein)
0.15
0.10
0.05
0.00
ns
**
ND
HFD
HFD + 3

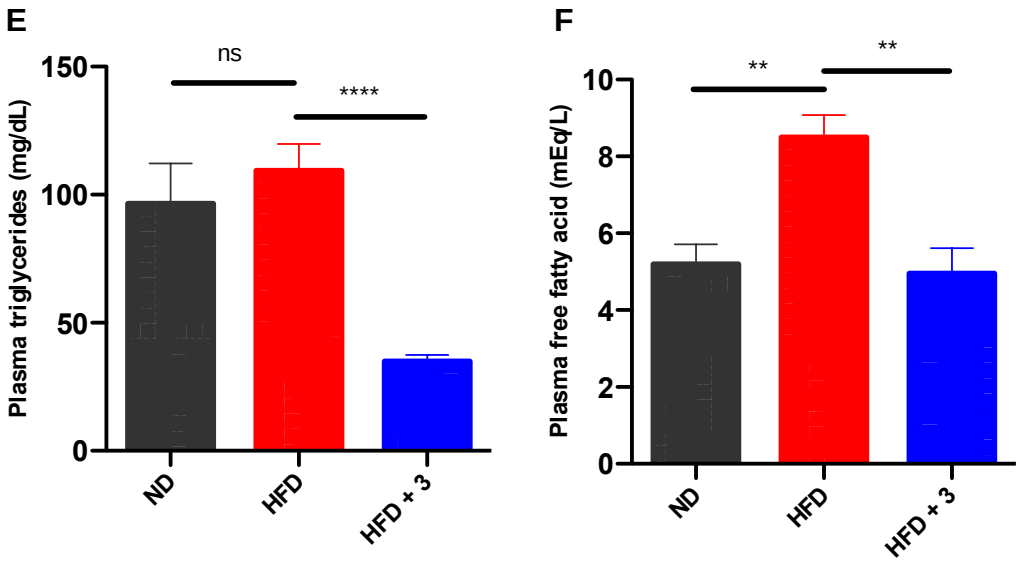

Figure 5. In vivo results of mice liver, lipid metabolism and SMS inhibitory activity. (A) Liver weight of the mice; (B) Representatives images of liver gross appearance; (C) Representatives images of Oil Red O staining (N = 3 mice per group); (D) Hepatic triglycerides; (E) Plasma triglycerides; (F) Plasma free fatty acids; (G) Conversion of NBD-Phosphocholine; (H) Conversion of NBD-Ceramide. Measurements were taken from distinct samples. Scale bar, 100 µm. Control: ND, normal chow diet & HFD, High fat diet; Test group: HFD + **3**, High fat diet with 0.1% of compound **3**. Data are presented as mean ± standard error of the mean (SEM); N = 7-8 mice per group. Statistical analysis was done by using t-test: (*) $P < 0.05$, (**) $P < 0.01$, (***) $P < 0.001$, (****) $P < 0.0005$, ns = no significant difference versus the control.

To further investigate the involvement of SMSs inhibitory activity *in vivo*, we then examined the lipidomics of the mouse liver by LC-MS/MS. Despite our expectations, total SM was increase and SM/ceramide ratio did not change in HFD + **3** as compared to control groups (**Figures 6 A-C**). It further remains unclear as to why sphingolipids analysis were not directly shown the SMS inhibitory activities of compound **3**. Herein, we showed that lipidomics could not be the suitable tool for obesity study *in vivo* in the case of compound **3** which exhibited multiple pharmacological activities and possibly affect the cell systems. Nevertheless, we found that SM and ceramide of (d18:1/C16:0) and (d18:1/C24:1) level were elevated than the rest (**Figures 6 D-E**).

Regards to our lipidomics findings, there are some factors may involve in the correspondence result. The results suggested that compound **3** may possibly act as a dual inhibitor which not only inhibits SMS activity but also involve in preventing the conversion of SM to ceramide through SMase. To support our findings, further evaluation of the SMase inhibitory activity of compound **3** are needed. Since lipid metabolism is highly regulated and complex whereby many stimuli and agents affect one or more enzymes, this might be a reasonable cause as to why increasing in total SM levels happens.

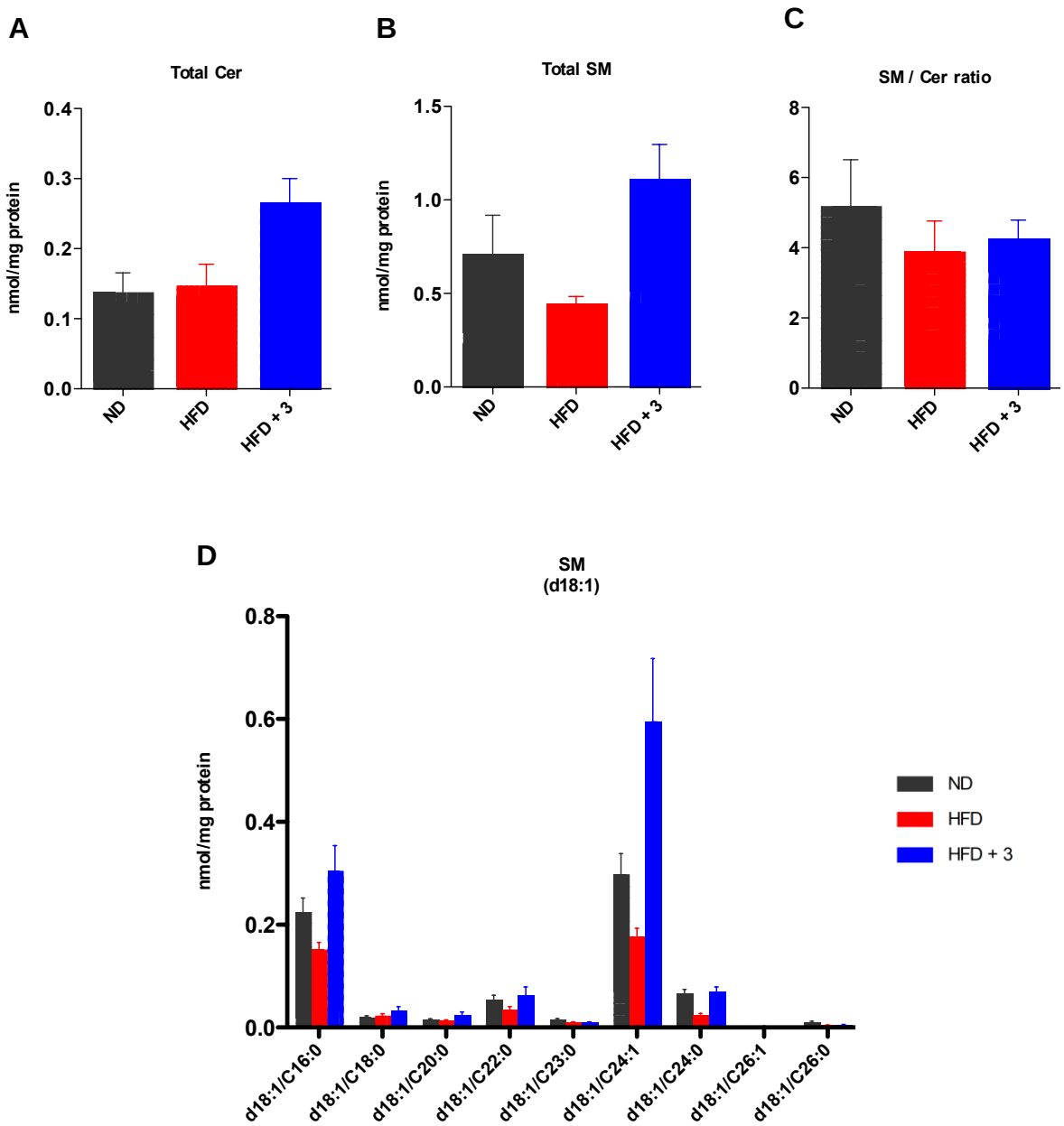

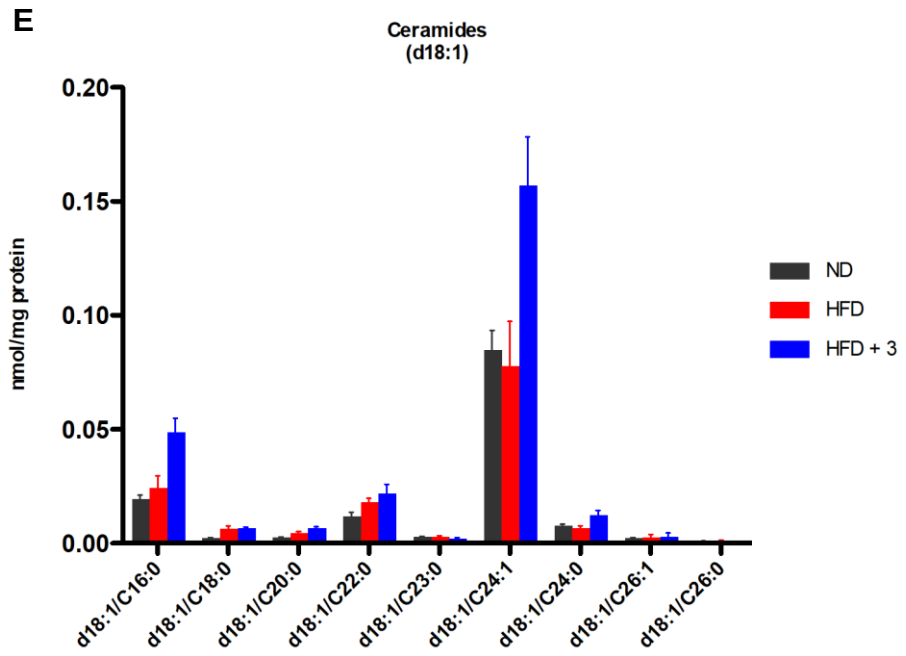

Figure 6. In vivo results of lipidomics analysis. (A) Total ceramide; (B) Total sphingomyelin; (C) Sphingomyelin : ceramide ratios; (D) Different types of sphingomyelin ; (E) Different types of ceramide. Measurements were taken from distinct samples. Scale bar, 100 µm. Control: ND, normal chow diet & HFD, High fat diet; Test group: HFD + **3**, High fat diet with 0.1% of compound **3**. Data are presented as mean ± standard error of the mean (SEM); *N* = 7-8 mice per group. Statistical analysis was done by using t-test: (*) $P < 0.05$, (**) $P < 0.01$, (***) $P < 0.001$, (****) $P < 0.0005$, ns = no significant difference versus the control.

Finally, we assessed the synthesis of DAG and SM via liver tissue lysate assays to further confirm the *in vivo* SMS inhibitory activities by compound **3**. Indeed, we have proved that for the first time, compound **3** as a natural SMS inhibitor, has significantly reduced the synthesis of the DAG and SM in the liver (**Figures 7A-B**). Herein, we underlined the *in vitro* and *in vivo* efficacies of compound **3** in its inhibition of the SMS2 enzyme and its putative mechanism involving the prevention of obesity. Interestingly, we demonstrated that compound **3** results in body weight reduction, improves glucose tolerance and lowers hepatic steatosis *in vivo*. Further studies on gene expression related to lipogenesis and gluconeogenesis are required to better understand the exact metabolism which is involved.

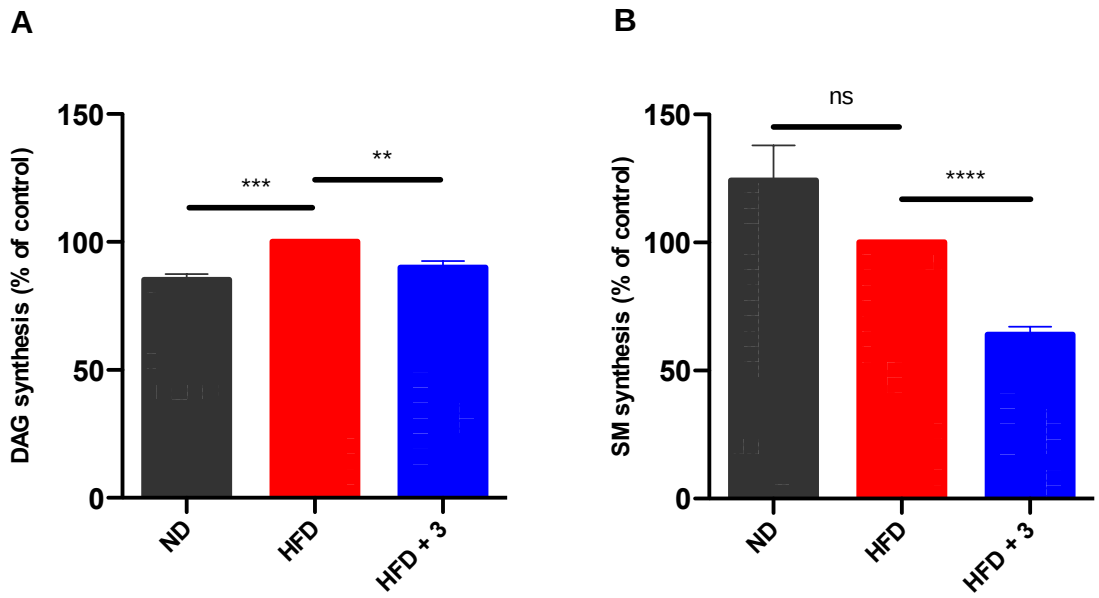

Figure 7. In vivo results of mice liver, lipid metabolism and SMS inhibitory activity. (A) Conversion of NBD-Phosphocholine; (B) Conversion of NBD-Ceramide. Measurements were taken from distinct samples. Scale bar, 100 µm. Control: ND, normal chow diet & HFD, High fat diet; Test group: HFD + **3**, High fat diet with 0.1% of compound **3**. Data are presented as mean ± standard error of the mean (SEM); *N* = 7-8 mice per group. Statistical analysis was done by using t-test: (*) $P < 0.05$, (**) $P < 0.01$, (***) $P < 0.001$, (****) $P < 0.0005$, ns = no significant difference versus the control.

Conclusion

In summary, malabaricone C (**3**), an acylphenol isolated from the fruits of *M. cinnamomea*, has been identified as a lead natural sphingomyelin inhibitor. Having the same mechanisms of action as the previously reported SMS knockout studies, malabaricone C was highly efficacious in preventing oleic acid uptake across the membrane which in turn reduced lipid droplet formation *in vitro*.[15] Malabaricone C was also found to be able to reduce body weight gain, improve glucose tolerance and decrease lipid accumulation in the liver *in vivo*, thus making this the first report involving a plant derived SMS inhibitor against high fat diet-induced obesity. Its non-toxic nature makes malabaricone C a suitable candidate for its further development as a new drug or medicinal supplement to treat and prevent obesity.

3.4 Experimental Section

General experimental method

All chemicals and solvents were obtained from commercial supplier and used without further purification. ^{1}H NMR (500 MHz) and ^{13}C NMR (125 MHz) spectra were recorded on a Varian Inova instrument at 25 °C in $CDCl_3$ and CD_3OD purchased from Cambridge Isotope Laboratories, Inc. (Tewksbury, USA). Chemical shifts (δ) are reported in ppm and coupling constant values (*J*) are in hertz relative to $CDCl_3$ (^{1}H, δ 7.26; ^{13}C, δ 77.00) or CD_3OD (^{1}H, δ 3.4, 4.8; ^{13}C, δ 49.3) and tetramethylsilane. The following abbreviations were used for signal multiplicities: s = singlet; d = doublet; t = triplet; q = quartet; p = pentet and m = multiplet. High Resolution Mass spectra (HRMS (ESI)) were obtained from AB sciex Triple TOF® 5600+ at Platform for Research on Biofunctional Molecules, Hokkaido University. Analytical TLC was performed on 0.2 mm silica gel plates (Merck 60 F-254). SiO_2 gel column chromatography was carried out using silica gel (Wakogel® N60, spherical, 38-100 μm) with air flashing. The purity of isolated compounds was determined by NMR, all the compounds have purity of >90-95%.

Plants material

Myristica cinnamomea King was collected from Johor, Malaysia in 2003. The plant was identified by Mr. Teo Leong Eng and a voucher specimen (KL 5043) was deposited at the University of Malaya herbarium.

Isolation of active compounds from *M. Cinnamomea*

Dried and powdered fruits (1.5 kg) of *M. cinnamomea* was extracted with ethyl acetate (5.0 L), at room temperature two times, yielding 263 g of a dark brown extract and checked for SMS assay. The active ethyl acetate extract (35 g) had higher inhibition activity against SMS and bioassay guided fractionation of the *M. cinnamomea* resulted in the isolation of malabaricones A-C (**1-3**) and malabaricone E (**4**). All isolated known compounds were confirmed by NMR spectroscopy, HRMS and having similar spectroscopic data with those reported in the literatures.[26,27] The yield obtained are as followed: Malabaricones A-C (5.58 g, 2.92 g, 6.04 g) and Malabaricone E (7.10 mg).

Malabaricone A (**1**) was obtained as a pale yellow, amorphous powder; HRMS (*m/z*): $[M + H]^+$, calculated for $C_{21}H_{27}O_3$: 327.1954; found : 327.1950. ^{1}H NMR (MeOH-d_4, 500 MHz): δ = 7.21 (2H, m), 7.18 (1H, t, J = 8.2 Hz), 7.15 (3H, m), 6.34 (2H, d, J = 8.2 Hz), 3.10 (2H, t, J = 7.3 Hz), 2.58 (2H, t, J = 7.3 Hz), 1.66 (2H, p, J = 7.3 Hz), 1.59 (2H, p, J = 7.3 Hz), 1.33 (8H, br s). ^{13}C NMR (MeOH-d_4, 125 MHz): δ = 209.8, 163.6, 163.6, 144.1, 137.0, 129.5, 129.5, 129.4, 129.4, 126.7, 111.5, 108.5, 108.5, 45.9, 37.1, 32.9, 30.8, 30.7, 30.6, 30.4, 25.9.

Malabaricone B (**2**) was obtained as a pale yellow, amorphous powder; HRMS (*m/z*): $[M + H]^+$, calculated for $C_{21}H_{27}O_4$: 343.1903; found : 343.1903. ^{1}H NMR (MeOH-d_4, 500 MHz): δ = 7.19 (1H, d, J =8.2 Hz), 6.97 (2H, d, J = 8.2 Hz), 6.67 (2H, d, J = 8.2 Hz), 6.33 (2H, d, J = 8.2 Hz), 3.11 (2H, t, J = 7.3 Hz), 2.49 (2H, t, J = 7.3 Hz), 1.67 (2H, p, J = 7.3 Hz), 1.55 (2H, p, J = 7.3 Hz), 1.34 (8H, br s). ^{13}C NMR (MeOH-d_4, 125 MHz): δ = 209.8, 163.6, 163.6, 144.1, 137.0, 129.5, 129.5, 129.4, 129.4, 126.7, 111.5, 108.5, 108.5, 45.9, 37.1, 32.9, 30.8, 30.7, 30.6, 30.4, 25.9.

Malabaricone C (**3**) was obtained as a yellow, amorphous powder; HRMS (*m/z*): $[M + H]^+$, calculated for $C_{21}H_{27}O_5$: 359.1853; found : 359.1862. ^{1}H NMR (MeOH-d_4, 500 MHz): δ = 7.19 (1H, d, J = 8.2 Hz), 6.65 (1H, d, J = 8.2 Hz), 6.60 (1H, d, J = 2.0 Hz), 6.47 (1H, dd, J = 8.2, 2.0 Hz), 6.34 (2H, d, J = 8.2 Hz), 3.11 (2H, t, J = 7.3 Hz), 2.44 (2H, t, J = 7.3 Hz), 1.67 (2H, p, J = 7.3 Hz), 1.54 (2H, p, J = 7.3 Hz), 1.33 (8H, br s). ^{13}C NMR (MeOH-d_4, 125 MHz): δ = 209.8, 163.6, 163.6, 146.1, 144.2, 137.0, 135.9, 120.8, 116.6, 116.3, 111.5, 108.5, 108.5, 45.9, 36.4, 33.1, 30.8, 30.7, 30.7, 30.4, 25.9.

Malabaricone E (**4**) was obtained as a yellow, amorphous powder; HRMS (*m/z*): $[M + H]^+$, calculated for $C_{21}H_{27}O_5$: 359.1853; found : 359.1861. ^{1}H NMR (MeOH-d_4, 400 MHz): δ = 6.97 (2H, d, J = 8.0 Hz), 6.67 (2H, d, J = 8.0 Hz), 5.80 (2H, s), 3.02 (2H, t, J = 8.0 Hz), 2.49 (2H, t, J = 8.0 Hz), 1.65 (2H, p, J = 8.0 Hz), 1.56 (2H, br t, J = 8.0 Hz), 1.33 (8H, br s). ^{13}C NMR (MeOH-d_4, 100 MHz): δ = 206.1, 164.6, 164.4, 164.4, 154.8, 133.5, 128.8, 128.8, 114.5, 114.5, 103.9, 94.3, 94.3, 43.4, 34.6, 31.6, 29.2, 29.2, 29.1, 28.9, 24.8.

Cell culture

The mouse embryonic fibroblast (tMEF) containing ZS/SMS1 and ZS/SMS2, WT-tMEF were presented from Prof. Igarashi (Lipid Bio Section, Faculty of Advanced Life Science, Hokkaido University). ZS cells was isolated from a SMS1, SMS2 double KO MEF, which was immortalized using SV40T antigen. ZS cells stably expressed SMS1 or SMS2, were named ZS/SMS1 and ZS/SMS2.[15] HepG2 cells were obtained from ATCC. Cells were cultured in dulbecco's modified eagle's medium (DMEM) supplemented with 10% (v/v) fetal bovine serum (FBS), 1% (v/v) penicillin with streptomycin at 34 °C in a 5% CO_2 incubator.

Measurement of SMSs inhibitory activity in cell lysates

Cell lysates were prepared as follows: ZS/SMS1 and ZS/SMS2 cells (protein concentration 0.1 µg/µL) were diluted by 20 mM Tris-buffer (pH 7.5) and sonicated. Aliquots of the cell lysates 100 µL were added with 1 µL of inhibitor of desired concentration and incubated at 37°C. After 30 min, the solutions were added with 1 µL of C6-NBD-ceramide (5 µM), and incubated for 3 h at 37°C. The reaction was stopped by addition of 400 µL of Methanol/Chloroform [1/2 (v/v)]; the mixture was shaken and centrifuged (1500 rpm x 5 min). The formation of C6-NBD-sphingomyelin was quantified by determination of the peak area of C6-NBD-sphingomyelin using high performance liquid chromatography (HPLC). A reverse phase HPLC assay using a JACSO HPLC system was developed for the quantitative analysis of the inhibitory activity. The system was equipped with a PU-2089 Plus and FP-2020 Plus set at λex = 470 nm and λem = 530 nm. A 50 x 4.6 YMC-Pack Diol-120-NP column (5-µm particle size) was used with mobile phase (IPA/hexane/water) at a flow rate of 1.0 mL/min.[33]

Measurement of SMSs inhibitory activity in cells

The tMEF cells were seeded at a density of 3.0×10^5 in 10 ml of DMEM medium containing 10% (v/v) fetal bovine serum (FBS), 1% (v/v) penicillin with streptomycin per 96 well-plate and cultured at 34 °C overnight. The medium was removed from the well-plate and 100 µl of inhibitor in medium containing 1% ethanol was added and incubated at 37 °C for 1 hour. The reaction then proceeds with an addition of 1 µl of C_6-NBD-ceramide (400 µM) in medium solution and incubated at 37 °C for 1 hour. The reaction mixture was removed and washed with 100 µl of PBS. The cell was digested with 20 µl of trypsin and incubated at 37 °C for 1 minute. Before transferring the whole amount of cell mixture to a deep well plate, 80 µl of PBS was added. The reaction was stopped and analyse in similar manner as previously described in cell lysate assays.

Animal care and experiments

All procedures were performed in accordance with guidelines by the animal research committee of Hokkaido University. Male C57BL/6 mice (five-week-old, Japan SLC Inc. Shizuoka, Japan) were housed in a temperature and humidity controlled cage (24 °C, 50% ± 10% relative humidity) with a 12 h light : dark cycle. The mice were sorted into 4 groups (n = 7-8 each) based on their body weight. The groups are as follows: 1) normal diet; vehicle control group (ND, 6.2% calories from fat, AIN-93M, Oriental Yeast Co., ltd, Japan), 2) high-fat diet; vehicle control group (HFD, 60% calories from fat, HFD-60, Oriental Yeast Co., ltd, Japan), and 3) HFD + 0.1% Compound 3 diet; treatment group. The mice were given free access to food ad libitum and water, meanwhile the weight change and feed intake were measured weekly. The animal experiments continued for 9 weeks. Body weight, blood glucose and liver function were recorded.

Tissue sampling

After treatment, animals were anaesthetized with ketamine and xylazine, blood was sampled from the hearts and perfused intracardially with 40 ml of saline (0.9% NaCI). Liver tissues were precisely dissected, weighed and snap-frozen in liquid nitrogen and stored at −80 °C until further analysis.

Histopathological examination

Sample of liver for each group were resected and fixed with 4% formaldehyde phosphate buffered with saline pH 7.4, then embedded in paraffin, sectioned, stained with Oil Red O staining and the images were captured by Axio Imager M2 (Zeiss).

Oral glucose tolerance test (OGTT)

Oral glucose tolerance test was performed by oral administration of glucose solution (1 mg/g) after overnight fasting. The level of blood glucose was measured using a glucose meter (Accu Check, Roche, Switzerland) before oral glucose load (0 min); 30, 60 and 120 minutes after oral glucose load. The data collected during OGTT was plotted and calculated by GraphPad Prism.

Biochemical analysis

Levels of blood and hepatic triglycerides (TG) and free fatty acids (FFA) were measured as previously described by using TG and FFA enzyme-linked immunosorbent assay (ELISA) kit from (Wako, Japan) following the manufacturer's instructions. The bioassay was conducted using a 96-well plate, and the absorbance was determined at 550 nm for FFA and 595 nm for TG using a microplate reader (Model 680, BIO-RAD, Japan).

Measurement of DAG and SM levels in liver tissues lysates

Liver samples were weighted, homogenized, and centrifuged to get supernatant as lysates solution. The reaction and analysis were similar as previously described in cell lysate assays. The DAG and SM levels were calculated by GraphPad.

Measurement of intracellular triglycerides and free fatty acid levels.

1 X 10^5 cells/well of HepG2 cells were seeded in a 12-well plate and incubated at 37 °C in 5% CO_2. The next day, the cells were treated with 1 mM of oleic acid in FBS-free medium. Cells were incubated for 1 day in a CO_2 incubator at 37 °C. Cells were washed with PBS and scraped to measure the triglycerides (TG) and free fatty acids (FFA) levels as previously described.

Immunofluorescence of lipid droplets from the oleic acid uptake.

1 X 10^5 cells/well of HepG2 cells were seeded in a 12-well plate and incubated at 37 °C in 5% CO_2. The next day, the cells were treated with 1 mM of oleic acid in FBS-free medium. Cells were incubated for 1 day in a CO_2 incubator at 37 °C. After washing with PBS, the cells were fixed with 4% of paraformaldehyde in PBS for 30 minutes. Subsequently, cells were washed with PBS and stained with 2.5 mg/ml of Nile red solution for 15 minutes. Next, cells were stained with DAPI solution for 2 minutes and continue washed with PBS. The images were captured using a fluorescence microscope BZ-X70 (Keyence, Osaka, Japan) and analysed using ImageJ.

Lipidomics of mice liver

Each piece of mouse liver samples were soaked in 3.5 mL of chloroform:methanol:water (1:2:0.5 by volume) and added 0.1 nmol of internal standard sphingolipids (ceramide (d18:1/C17:0), glucosylceramide (d18:1/C12:0), and sphingomyelin (d18:1/C17:0)). After slight sonication, lipids were extracted at 48 ^{o}C for 2 hours. 70 μL of 10 M sodium hydroxide solution was added to lipids extract to degrade glycerolipids and incubated at 37 ^{o}C for 2 hours. Phase separations were achieved by adding water (1.7 mL) and chroloform (1.6 mL). Lower organic phase was transferred to test tubes and residual lipids were re-extracted from upper phase with 2 mL of chloroform. Recovered lipid extracts were dry out under nitrogen stream and lipid extracts were dissolved with 150 μL of acetonitrile:methanol (19:1 by volume). LC-MS/MS analysis was carried out with a TripleTOF 5600 system (AB SCIEX, Foster City, California, USA) in electrospray ionization (ESI) positive mode[MS1)]. Lipid samples were injected onto an InertSustain NH_2 hydrophilic interaction chromatography (HILIC) column (particle size, 5 μm; diameter, 2.1 mm; length, 100 mm; GL Science). Sphingolipids were eluted at 0.13 mL/min over a 45 min gradient referred and slight modified to literature[MS1, MS2)]. Each sphingolipid species was identified by their retention times and typical product ions (ceramide and glucosylceramide for *m/z* 264.3 and sphingomyelin for *m/z* 184.1).

1H NMR of Malabaricone A (1)

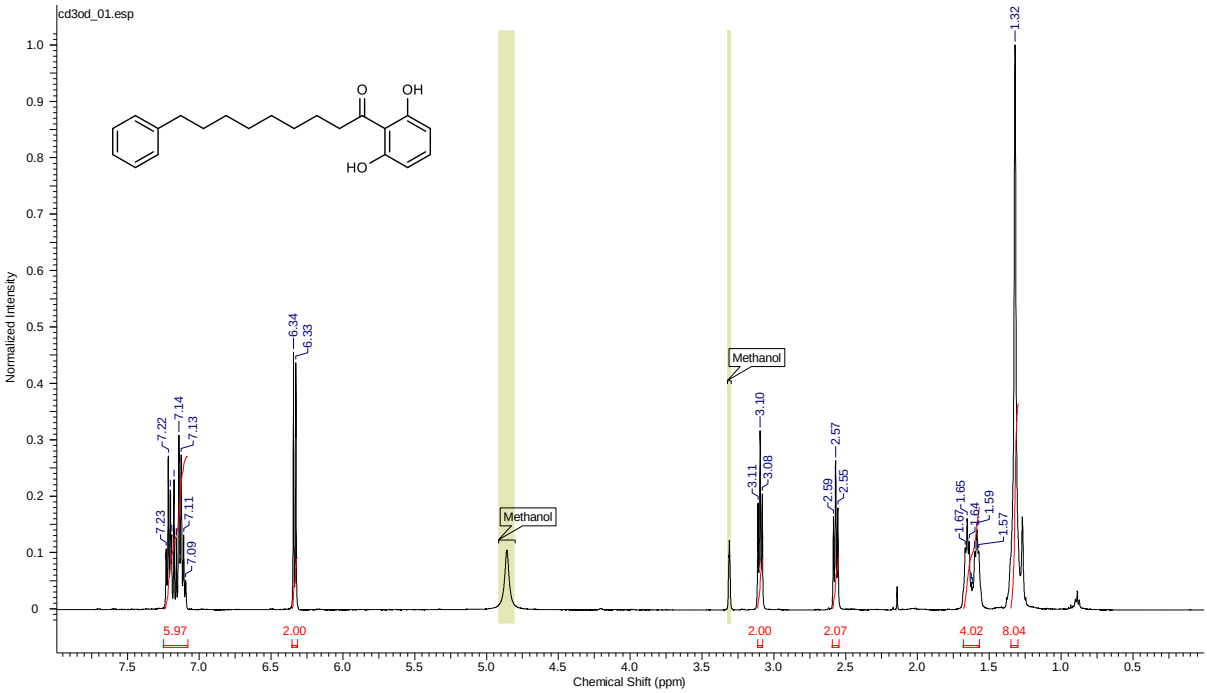

1H NMR of Malabaricone B (2)

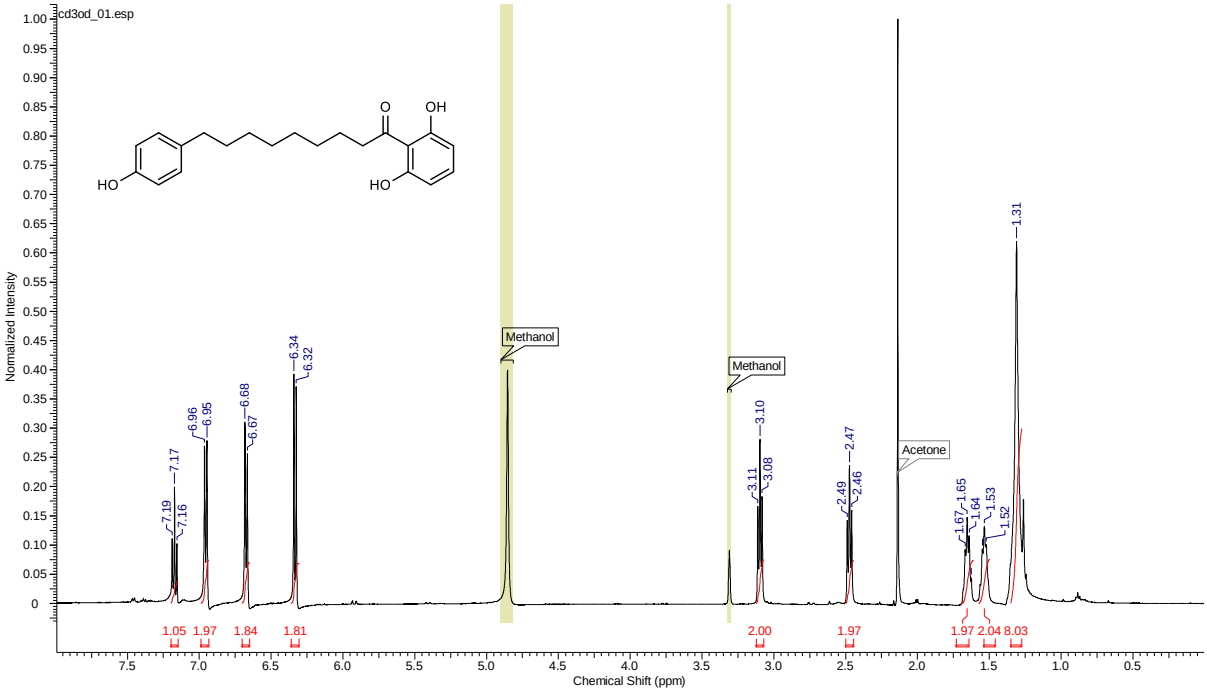

1H NMR of Malabaricone C (3)

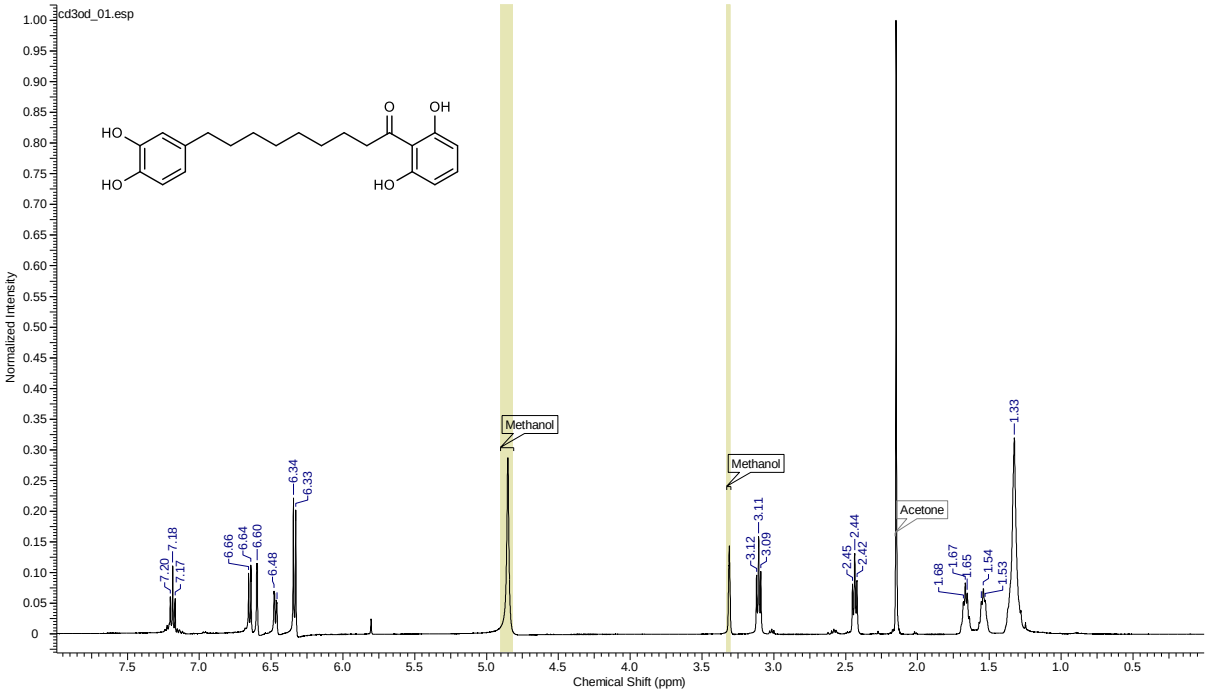

1H NMR of Malabaricone E (4)

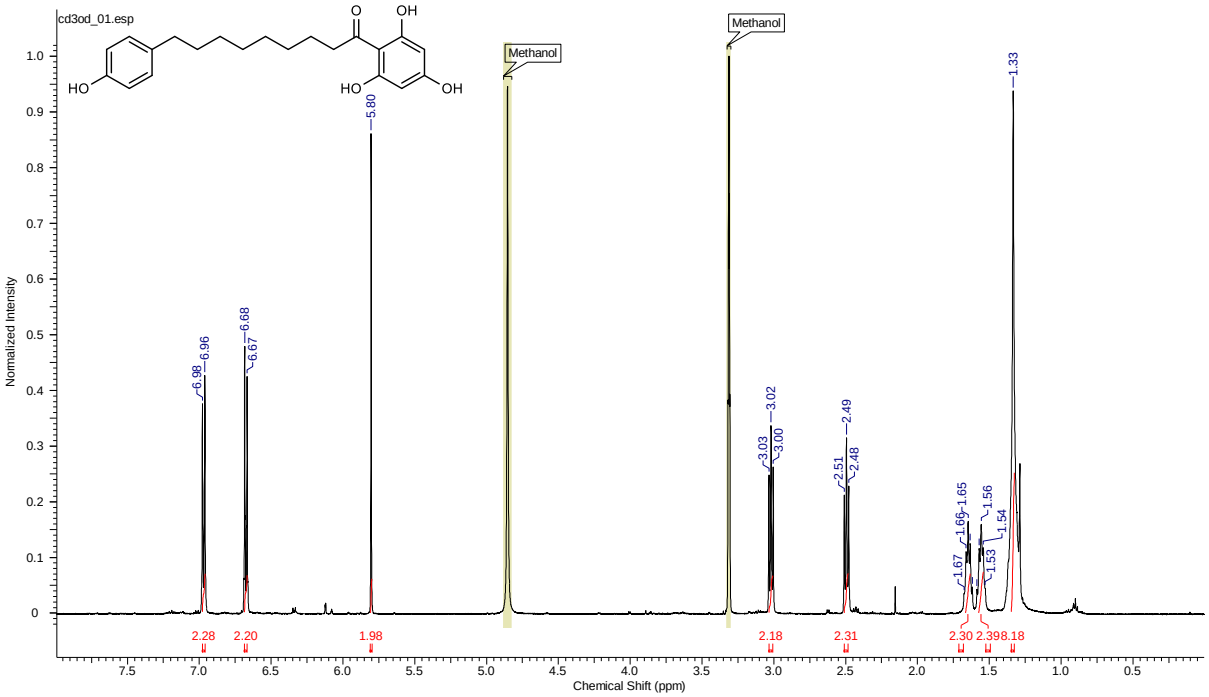

3.5 References

(1) Jaacks, L. M.; Vandevijvere, S.; Pan, A.; McGowan, C. J.; Wallace, C.; Imamura, F.; Mozaffarian, D.; Swinburn, B.; Ezzati, M. The Obesity Transition: Stages of the Global Epidemic. *lancet. Diabetes Endocrinol.* **2019**, *7* (3), 231–240.

(2) Wang, K.; Bao, L.; Zhou, N.; Zhang, J.; Liao, M.; Zheng, Z.; Wang, Y.; Liu, C.; Wang, J.; Wang, L.; et al. Structural Modification of Natural Product Ganomycin I Leading to Discovery of a α-Glucosidase and HMG-CoA Reductase Dual Inhibitor Improving Obesity and Metabolic Dysfunction in Vivo. *J. Med. Chem.* **2018**, *61* (8), 3609–3625.

(3) De Haas, E. C.; Oosting, S. F.; Lefrandt, J. D.; Wolffenbuttel, B. H. R.; Sleijfer, D. T.; Gietema, J. A. The Metabolic Syndrome in Cancer Survivors. *Lancet Oncol.* **2010**, *11* (12), 193–203.

(4) Goto-Inoue, N.; Yamada, K.; Inagaki, A.; Furuichi, Y.; Ogino, S.; Manabe, Y.; Setou, M.; Fujii, N. L. Lipidomics Analysis Revealed the Phospholipid Compositional Changes in Muscle by Chronic Exercise and High-Fat Diet. *Sci. Rep.* **2013**, *3* (1), 3267.

(5) Lee, Y.; Basith, S.; Choi, S. Recent Advances in Structure-Based Drug Design Targeting Class A G Protein-Coupled Receptors Utilizing Crystal Structures and Computational Simulations. *J. Med. Chem.* **2018**, *61* (1), 1–46.

(6) Overington, J. P.; Al-Lazikani, B.; Hopkins, A. L. How Many Drug Targets Are There? *Nat. Rev. Drug Discov.* **2006**, *5* (12), 993–996.

(7) Hopkins, A. L.; Groom, C. R. The Druggable Genome. *Nat. Rev. Drug Discov.* **2002**, *1* (9), 727–730.

(8) Berridge, G.; Chalk, R.; D'Avanzo, N.; Dong, L.; Doyle, D.; Kim, J.-I.; Xia, X.; Burgess-Brown, N.; deRiso, A.; Carpenter, E. P.; et al. High-Performance Liquid Chromatography Separation and Intact Mass Analysis of Detergent-Solubilized Integral Membrane Proteins. *Anal. Biochem.* **2011**, *410* (2), 272–280.

(9) Huitema, K.; van den Dikkenberg, J.; Brouwers, J. F. H. M.; Holthuis, J. C. M. Identification of a Family of Animal Sphingomyelin Synthases. *EMBO J.* **2004**, *23* (1), 33–44.

(10) Yamaoka, S.; Miyaji, M.; Kitano, T.; Umehara, H.; Okazaki, T. Expression Cloning of a Human CDNA Restoring Sphingomyelin Synthesis and Cell Growth in Sphingomyelin Synthase-Defective Lymphoid Cells. *J. Biol. Chem.* **2004**, *279* (18), 18688–18693.

(11) Ullman, M. D.; Radin, N. S. The Enzymatic Formation of Sphingomyelin from Ceramide and Lecithin in Mouse Liver. *J. Biol. Chem.* **1974**, *249* (5), 1506–1512.

(12) Merrill, A. H.; Jones, D. D. An Update of the Enzymology and Regulation of Sphingomyelin Metabolism. *Biochim. Biophys. Acta - Lipids Lipid Metab.* **1990**, *1044* (1), 1–12.

(13) Bienias, K.; Fiedorowicz, A.; Sadowska, A.; Prokopiuk, S.; Car, H. Regulation of

Sphingomyelin Metabolism. *Pharmacol. Reports* **2016**, *68* (3), 570–581.

(14) Hannun, Y. A. Functions of Ceramide in Coordinating Cellular Responses to Stress. *Science* **1996**, *274* (5294), 1855–1859.

(15) Mitsutake, S.; Zama, K.; Yokota, H.; Yoshida, T.; Tanaka, M.; Mitsui, M.; Ikawa, M.; Okabe, M.; Tanaka, Y.; Yamashita, T.; et al. Dynamic Modification of Sphingomyelin in Lipid Microdomains Controls Development of Obesity, Fatty Liver, and Type 2 Diabetes. *J. Biol. Chem.* **2011**, *286* (32), 28544–28555.

(16) Yuyama, K.; Sun, H.; Mitsutake, S.; Igarashi, Y. Sphingolipid-Modulated Exosome Secretion Promotes Clearance of Amyloid-β by Microglia. *J. Biol. Chem.* **2012**, *287* (14), 10977–10989.

(17) Hanamatsu, H.; Ohnishi, S.; Sakai, S.; Yuyama, K.; Mitsutake, S.; Takeda, H.; Hashino, S.; Igarashi, Y. Altered Levels of Serum Sphingomyelin and Ceramide Containing Distinct Acyl Chains in Young Obese Adults. *Nutr. Diabetes* **2014**, *4* (10), e141.

(18) Kim, Y.-J.; Greimel, P.; Hirabayashi, Y. GPRC5B-Mediated Sphingomyelin Synthase 2 Phosphorylation Plays a Critical Role in Insulin Resistance. *iScience* **2018**, *8*, 250–266.

(19) Yuyama, K.; Mitsutake, S.; Igarashi, Y. Pathological Roles of Ceramide and Its Metabolites in Metabolic Syndrome and Alzheimer's Disease. *Biochim. Biophys. Acta - Mol. Cell Biol. Lipids* **2014**, *1841* (5), 793–798.

(20) Ohnishi, T.; Hashizume, C.; Taniguchi, M.; Furumoto, H.; Han, J.; Gao, R.; Kinami, S.; Kosaka, T.; Okazaki, T. Sphingomyelin Synthase 2 Deficiency Inhibits the Induction of Murine Colitis-Associated Colon Cancer. *FASEB J.* **2017**, *31* (9), 3816–3830.

(21) Fan, Y.; Shi, F.; Liu, J.; Dong, J.; Bui, H. H.; Peake, D. A.; Kuo, M.-S.; Cao, G.; Jiang, X.-C. Selective Reduction in the Sphingomyelin Content of Atherogenic Lipoproteins Inhibits Their Retention in Murine Aortas and the Subsequent Development of Atherosclerosis. *Arterioscler. Thromb. Vasc. Biol.* **2010**, *30* (11), 2114–2120.

(22) Swamy, M. M. M.; Murai, Y.; Ohno, Y.; Jojima, K.; Kihara, A.; Mitsutake, S.; Igarashi, Y.; Yu, J.; Yao, M.; Suga, Y.; et al. Structure-Inspired Design of a Sphingolipid Mimic Sphingosine-1-Phosphate Receptor Agonist from a Naturally Occurring Sphingomyelin Synthase Inhibitor. *Chem. Commun.* **2018**, *54* (90), 12758–12761.

(23) Liu, Z. H.; Zeng, S. Cytotoxicity of Ginkgolic Acid in HepG2 Cells and Primary Rat Hepatocytes. *Toxicol. Lett.* **2009**, *187* (3), 131–136.

(24) Jiang, L.; Si, Z.-H.; Li, M.-H.; Zhao, H.; Fu, Y.-H.; Xing, Y.-X.; Hong, W.; Ruan, L.-Y.; Li, P.-M.; Wang, J.-S. 1H NMR-Based Metabolomics Study of Liver Damage Induced by Ginkgolic Acid (15:1) in Mice. *J. Pharm. Biomed. Anal.* **2017**, *136*, 44–54.

(25) Seidemann, J. World Spice Plants: Economic Usage, Botany, Taxonomy.; Springer-Verlag, 2005; pp 215–248.

(26) Purushothaman, K. K.; Sarada, A.; Connolly, J. D. Malabaricones A–D, Novel

Diarylnonanoids from Myristica Malabarica Lam (Myristicaceae). *J. Chem. Soc., Perkin Trans. 1* **1977**, *0* (5), 587–588.

(27) Abdul Wahab, S. M.; Sivasothy, Y.; Liew, S. Y.; Litaudon, M.; Mohamad, J.; Awang, K. Natural Cholinesterase Inhibitors from Myristica Cinnamomea King. *Bioorg. Med. Chem. Lett.* **2016**, *26* (15), 3785–3792.

(28) Banerjee, D.; Maity, B.; Bandivdeker, A. H.; Bandyopadhyay, S. K.; Chattopadhyay, S. Angiogenic and Cell Proliferating Action of the Natural Diarylnonanoids, Malabaricone B and Malabaricone C during Healing of Indomethacin-Induced Gastric Ulceration. *Pharm. Res.* **2008**, *25* (7), 1601–1609.

(29) Riju, A.; Sithara, K.; Nair, S. S.; Shamina, A.; Eapen, S. J. In Silico Screening Major Spice Phytochemicals for Their Novel Biological Activity and Pharmacological Fitness. *J. Bioequiv. Availab.* **2009**, *01* (02), 1–11.

(30) Zhang, L.; Wang, D.; Wen, M.; Du, L.; Xue, C.; Wang, J.; Xu, J.; Wang, Y. Rapid Modulation of Lipid Metabolism in C57BL/6J Mice Induced by Eicosapentaenoic Acid-Enriched Phospholipid from Cucumaria Frondosa. *J. Funct. Foods* **2017**, *28*, 28–35.

(31) Murase, T.; Nagasawa, A.; Suzuki, J.; Hase, T.; Tokimitsu, I. Beneficial Effects of Tea Catechins on Diet-Induced Obesity: Stimulation of Lipid Catabolism in the Liver. *Int. J. Obes.* **2002**, *26* (11), 1459–1464.

(32) Diehl, A. M. Fatty Liver, Hypertension, and the Metabolic Syndrome. *Gut* **2004**, *53* (7), 923–924.

(33) Swamy, M. M. M.; Murai, Y.; Ohno, Y.; Jojima, K.; Kihara, A.; Mitsutake, S.; Igarashi, Y.; Yu, J.; Yao, M.; Suga, Y.; et al. Structure-Inspired Design of a Sphingolipid Mimic Sphingosine-1-Phosphate Receptor Agonist from a Naturally Occurring Sphingomyelin Synthase Inhibitor. *Chem. Commun.* **2018**, *54* (90), 12758–12761.

Acknowledgments

Firstly, I would like to express my sincere gratitude to my supervisor Professor Kenji Monde for the continuous support of my doctoral study and related research, for his patience, motivation, and immense knowledge. His guidance helped me in all the time of research and writing of this thesis. I could not have imagined having a better advisor and mentor for my Ph.D study.

Besides my advisor, I would like to thank the rest of my thesis committee: Prof. Demura Makoto, Prof. Shin-Ichiro Nishimura, Associate Prof. Kohei Yuyama and Dr. Yuta Murai for their insightful comments and encouragement, but also for the inspiring question which incented me to widen my research from various perspectives.

My sincere thanks also goes to Prof. Khalijah Awang, Prof. Yasuyuki Igarashi, Dr. Yasodha Sivasothy, Dr. Sun and Dr. Tohru Taniguchi who provided me an opportunity to join their team and gave access to the laboratory and research facilities. Without they precious support it would not be possible to conduct this research.

I thank my fellow labmates (laboratory of molecular chemical biology) in for the stimulating discussions, and for all the fun and jokes we have had in the last three years. In particular, I am grateful to Yoshiko Suga, Prof. Masaki Anetai, Prof. Orito Kazuhiko and Keiko Abe for their tremendous support and help during my research activity.

Last but not the least, I would like to thank my family and my best friends (you know who you are) for supporting me spiritually throughout my Ph.D study and my life in general.

Publications

1. Papers (related to Doctoral Dissertation)

(1) **Muhamad Aqmal Othman**, Kohei Yuyama, Yuta Murai, Yasuyuki Igarashi, Daisuke Mikami, Yasodha Sivasothy, Khalijah Awang, and Kenji Monde. "Malabaricone C as natural sphingomyelin synthase inhibitor against diet-induced obesity and its lipid metabolism in mice" *ACS Med. Chem. Lett.* 2019, acsmedchemlett.9b00171. (Cover Journal)

2. Papers (Others)

(1) **Muhamad Aqmal Othman**, Yasodha Sivasothy, Chung Yeng Looi, Abdulwali Ablat, Jamaludin Mohamad, Marc Litaudon and Khalijah Awang. "Acylphenols and dimeric acylphenols from *Myristica maxima* Warb". *Fitoterapia*, 2016, 111, 12-17.

(2) Yasodha Sivasothy, Thiba Krishnan, Kok Gan Chan, Siti Mariam Abdul Wahab, **Muhamad Aqmal Othman**, Marc Litaudon and Khalijah Awang. "Quorum Sensing Inhibitory Activity of Giganteone A from *Myristica cinnamomea* King against *Escherichia coli* Biosensors". *Molecules*, 2016, 21, 391